OPEN ACCESS

Tumor Immunity REVIEW

Heterogeneity, immunological mechanisms and translational prospects of tertiary lymphoid structures in cancer therapy

Junjie Zheng,[1] Hui Huang,[1] Wanqiao Li,[1] Shijia Li,[1] Jialin Liu,[1] Zhihao Lu,[2,*] Cihui Yan,[3,*] and Wencheng Zhang[1,*]

*Correspondence: pppeirain@126.com (Z.L.); cihuiyan@tmu.edu.cn (C.Y.); wczhang@tmu.edu.cn (W.Z.)

Received: March 3, 2026; Accepted: April 23, 2026; Published Online: April 25, 2026; https://doi.org/10.59717/j.xinn-oncol.2026.100011

GRAPHICAL ABSTRACT

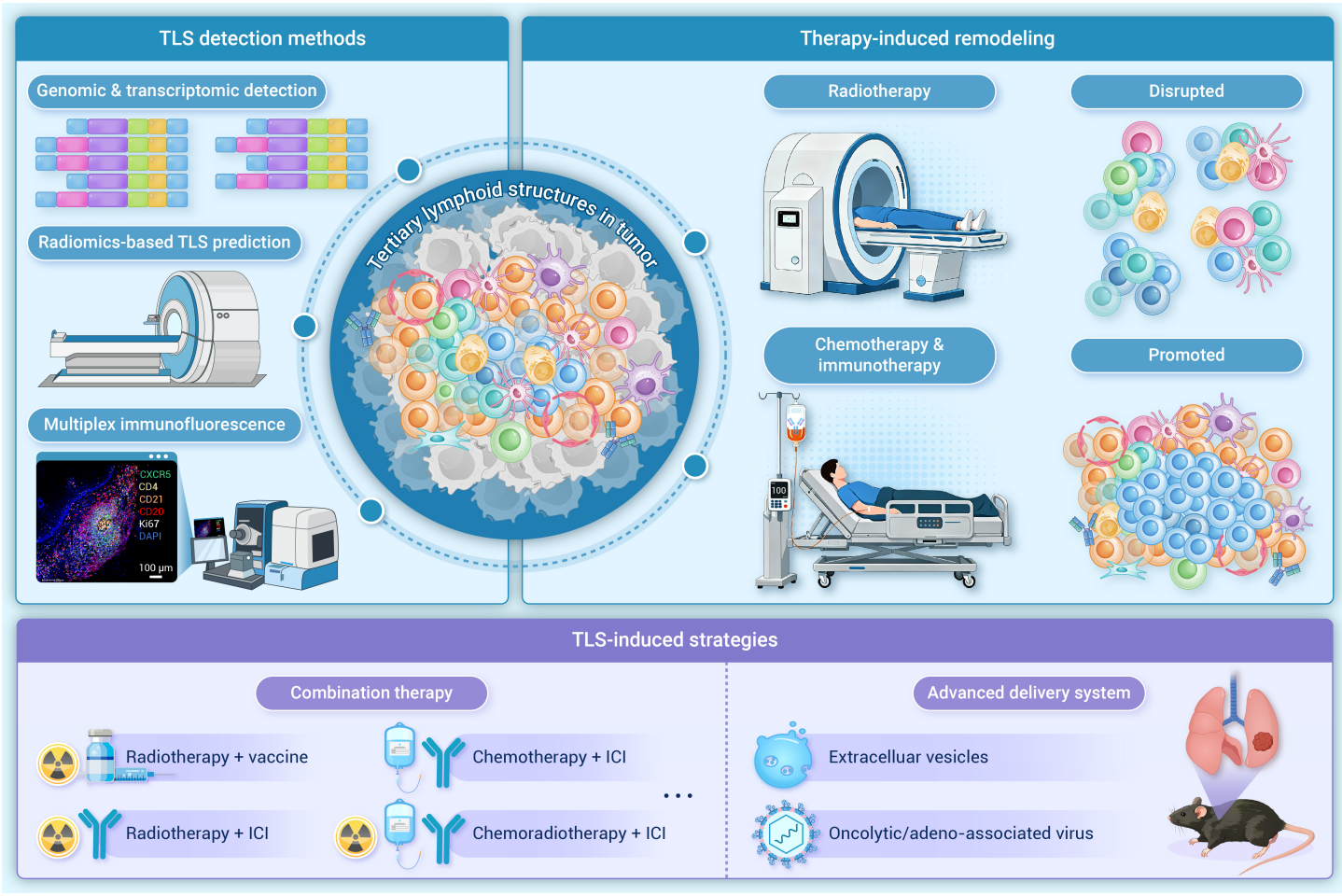

PUBLIC SUMMARY

- Tertiary lymphoid structures are organized immune niches that can shape cancer therapy outcomes.
- Their impact depends on maturation, location, and effector-versus-suppressive immune balance.
- Chemotherapy, radiotherapy, and immunotherapy can remodel tertiary lymphoid structures over time.
- Standardized tertiary lymphoid structure assessment may improve biomarkers and combination therapy.

REVIEW Tumor Immunity

www.the-innovation.org/the-innovation-oncology

Heterogeneity, immunological mechanisms and translational prospects of tertiary lymphoid structures in cancer therapy

Junjie Zheng,[1] Hui Huang,[1] Wanqiao Li,[1] Shijia Li,[1] Jialin Liu,[1] Zhihao Lu,[2,*] Cihui Yan,[3,*] and Wencheng Zhang[1,*]

[1]Department of Radiation Oncology, Tianjin Medical University Cancer Institute and Hospital, National Clinical Research Center for Cancer, Key Laboratory of Cancer Prevention and Therapy, Tianjin's Clinical Research Center for Cancer, Tianjin 300060, China

[2]Key laboratory of Carcinogenesis and Translational Research (Ministry of Education/Beijing), Department of Gastrointestinal Oncology, Peking University Cancer Hospital & Institute, Beijing 100142, China

[3]Department of Immunology, Tianjin Medical University Cancer Institute & Hospital, National Clinical Research Center for Cancer, Key Laboratory of Cancer Immunology and Biotherapy, Tianjin's Clinical Research Center for Cancer, Tianjin 300060, China

*Correspondence: pppeirain@126.com (Z.L.); cihuiyan@tmu.edu.cn (C.Y.); wczhang@tmu.edu.cn (W.Z.)

Received: March 3, 2026; Accepted: April 23, 2026; Published Online: April 25, 2026; https://doi.org/10.59717/j.xinn-oncol.2026.100011

Citation: Zheng J., Huang H., Li W., et al. (2026). Heterogeneity, immunological mechanisms and translational prospects of tertiary lymphoid structures in cancer therapy. *The Innovation Oncology* **1**:100011.

Tumor-associated tertiary lymphoid structures (TA-TLS) represent ectopic lymphoid neogenesis within chronically inflamed tumors and are increasingly linked to response to immune checkpoint blockade (ICB) and other anticancer therapies. However, TLS are not uniformly beneficial: their immune outputs vary with maturation, spatial niche (intratumoral, invasive margin, or peritumoral), and the balance between effector programs and suppressive modules. This heterogeneity, together with inconsistent definitions and measurement approaches, has limited cross-cohort comparability and slowed translation of TLS into reliable biomarkers and therapeutic targets. In this review, we synthesize key pathways governing TLS induction, formation, and maturation, emphasizing vascular and stromal scaffold requirements that enable lymphocyte recruitment and compartmentalization. We summarize and reconcile existing TLS classification frameworks across tumor types, and integrate mechanistic interactions among T cells, B cells, dendritic cells, myeloid populations, and stromal elements that shape TLS "quality" and immunological function. Importantly, we highlight therapy-induced TLS remodeling as a dynamic process influenced by chemotherapy, radiotherapy dose/fractionation and sequencing, anti-angiogenic strategies, and ICB itself—helping explain divergent clinical associations and suggesting time-ordered opportunities for intervention. Finally, we discuss multimodal approaches for standardized TLS assessment and outline emerging strategies to safely engineer high-quality TLS to enhance antitumor immunity and rationalize combination regimens.

INTRODUCTION

Although immune checkpoint blockade (ICB) has produced durable survival benefits in multiple tumor types, the overall response rate remains highly contingent on tumor lineage and the baseline state of the tumor microenvironment (TME), and both primary and acquired resistance are common.[1] Effective antitumor immunity requires coordinated completion of a series of steps. These include antigen release, antigen presentation, priming and expansion, trafficking and infiltration, and effector mediated tumor cell elimination. In solid tumors, constraints at both the initiation and the infiltration ends frequently coexist, resulting in a resistance landscape characterized by limited priming, insufficient replenishment, and T-cell exhaustion.[2] Therefore, rebuilding high-quality antigen presentation and coordinated T-B cell networks within tumors remains central to the next phase of cancer immunotherapy development. Leveraging this biology can enable clinically actionable stratification and rational combination regimens.[3]

Tumor-associated tertiary lymphoid structures (TA-TLSs) are a manifestation of ectopic lymphoid neogenesis in chronically inflamed tissues. They can arise intratumorally or peritumorally as structured immune units that include a T-cell zone coupled to dendritic cell activity and a B-cell follicle with germinal center like features. Accordingly, they are frequently conceptualized as potential in situ amplifiers of adaptive immunity.[4] However, TLS is not inherently synonymous with beneficial immune infiltration. TLS driven immune outputs can be substantially redirected in both magnitude and direction. Key factors include maturation state, ranging from early lymphoid aggregates to germinal center positive TLS, spatial niche (intratumoral, invasive margin, or peritumoral), and immunoregulatory modules such as regulatory T cells (Treg) or follicular regulatory T cell (Tfr) enrichment and myeloid suppression.[5] In addition, TLS definitions, staging criteria, and measurement methods are not well standardized across studies, which limits comparisons between cohorts and weakens the evidence for TLS as reliable prognostic or predictive biomarkers.[6] How different functional areas inside TLS (the T-zone and dendritic-cell axis, the B and T interface, and inhibitory areas) are organized, and how they causally relate to T-cell lineages (for example, precursor-exhausted vs terminally exhausted states), is still not fully resolved, so many mechanistic links remain mainly correlational.[3] Therapies such as ICB, chemotherapy and radiotherapy can reshape TLS formation and maturation over time, but longitudinal human data that clearly describe how baseline TLS differ from therapy-induced TLS in timing, structural quality, and immune-memory output remain limited.[7] Finally, we still lack safe and controllable ways to induce or boost "high-quality TLS" (not just increase lymphocyte aggregates) and to combine TLS induction with existing immunotherapies using widely usable engineering approaches and prospective clinical validation paths.[8]

As a starting point, this review outlines key pathways underlying TA-TLS induction, formation, and maturation, with an emphasis on vascular and stromal scaffold requirements. We then summarize existing TLS classification systems and discuss sources of consistency and divergence across tumor types. Next, we analyze how TLS may shift toward immune amplification or immune suppression based on the balance between effector and inhibitory modules. We integrate T-cell, B-cell, myeloid, and stromal interactions, and highlight cell-lineage signals most consistently linked to ICB responsiveness. We also examine treatment-induced remodeling of TLS as a dynamic, time-dependent process. We cover how chemotherapy can induce, reshape, or damage TLS depending on regimen and immune context, and how radiotherapy effects vary with dose, fractionation, treated volume, and sequencing. We further discuss how ICB can remodel TLS. We then review preclinical strategies to actively induce TLS or promote more mature, functional TLS to improve responses to immunotherapy. Finally, we synthesize detection strategies spanning digital pathology, bulk and single-cell transcriptomics, spatial omics, and radiomics, emphasizing that standardized labeling, cross-center generalizability, and incorporation of maturation and functional modules into scoring frameworks are critical for clinical translation.

INITIATION, FORMATION, AND MATURATION OF TA-TLS

Under pathological conditions such as chronic inflammation and cancer, non-lymphoid tissues can undergo ectopic lymphoid neogenesis and form TLS. TLS formation partly reuses key pathways from secondary lymphoid organ (SLO) development, especially the LTβR pathway, homeostatic chemokines, stromal scaffolds, and high endothelial venules (HEV)-like vascular programs. However, unlike stable SLOs that are set during embryonic development, TLS initiation signals rely more on local and long-lasting stimulation, which leads to strong plasticity and tissue specificity.[3,9,10] In temporal terms, SLOs are mostly formed during embryogenesis and remain stable afterward.[9] In contrast, TLS form after birth in response to persistent antigen stimulation or chronic inflammation, vary widely depending on inflammation strength and tissue context, and can partly regress when stimulation decreases.[3,10]

TLS initiation is typically preceded by a pro-inflammatory and recruitment program that establishes local 'permissive conditions' for cellular aggregation. In tumors, cell death and therapy-associated DNA damage and innate immune activation can engage the cyclic GMP-AMP synthase (cGAS)- stimulator of interferon gene (STING) axis, inducing type I interferons and recruitment programs that facilitate TLS initiation. In murine models, synergistic activation of STING and LTβR signaling promotes intratumoral HEV programming and TLS formation with germinal-center–like features.[11–13]

In parallel, the canonical lymphoid tissue inducer (LTi)–lymphoid tissue organizer (LTo) interaction paradigm from developmental immunology provides a prototype for organized lymphoid circuits. LTi cells are specialized immune cells that deliver lymphotoxin-family signals, whereas LTo cells are stromal organizer cells that respond by upregulating chemokines, adhesion molecules, and reticular scaffold programs required for lymphoid tissue assembly. SLO development depends on LTi cells (often classified within group 3 innate lymphoid cells (ILC3s) and expressing membrane-bound lymphotoxin $LT\alpha_1\beta_2$) interacting with LTβR-expressing LTo stromal cells.[9] LTβR is a member of the TNF receptor family. It can be activated by $LT\alpha_1\beta_2$ or LIGHT (TNFSF14, a TNF-superfamily ligand).[9,14] and can activate both canonical and non-canonical NF-κB pathways. The latter commonly proceeds via NIK-mediated processing of p100 to p52, nuclear translocation of the p52–RelB complex, and induction of organizer-associated gene programs that promote LTo maturation.[14] Meanwhile, the canonical pathway typically depends on the IKK complex to trigger IκB degradation, enabling rapid nuclear entry of RelA/p50 and preferentially amplifying early inflammatory and adhesion-molecule programs.[15] During TLS organization, the non-canonical NF-κB pathway (NIK, p52, and RelB) is usually the key downstream arm of LTβR. It drives and maintains chemokines such as CXCL13 and CCL19/CCL21 and related adhesion molecules, which support compartment formation and follicle development. The canonical NF-κB pathway (RelA/p50) helps create a microenvironment that supports cell recruitment and adhesion, and it works together with the non-canonical pathway to promote TLS maturation.[16–18]

Importantly, in TA-TLS, the cellular sources of 'LTi-like' and 'LTo-like' activities are more heterogeneous.[10] Beyond classical LTi cells, multiple immune cell types have been reported to provide $LT\alpha_1\beta_2$ or related TNF-family ligands with LTi-like functions in different models, including ILC2s,[19] Th17 cells,[20] follicular helper T cells (Tfh cells),[21,22] $CD8^+$ T cells,[23] B cells,[23] and DCs,[10] innate immune triggers such as TLR agonists can also promote tumor TLS formation in selected settings.[24] Correspondingly, 'LTo-like' cells are typically non-hematopoietic stromal cells or endothelial cells capable of responding to LTβR/TNFR signals by upregulating CXCL13, CCL19/CCL21, and adhesion programs while forming podoplanin$^+$ reticular scaffolds that transform diffuse infiltrates into compartmentalized structures.[10] Both animal models and human studies suggest that cancer-associated fibroblasts (CAFs) or specific fibroblast lineages can acquire LTo-like phenotypes and contribute to TLS organization, such as TNFR-driven organizer features in melanoma models and CCL19-secreting fibroblast programs that promote lymphocyte migration toward TLS in colorectal liver metastases.[23,25]

During organizational development, Stromal cells can secrete IL-7. IL-7 is thought to initiate tumor TLS neogenesis by sustaining and expanding LTi cells, thereby promoting the LTα1β2–LTβR feed-forward program that triggers early lymphoid chemokine cues.[26] IL-17, mainly from Th17/γδ T cells, promotes tumor TLS formation by activating IL-17R$^+$ LTo.[5,27] Mature LTo cells upregulate homeostatic chemokines and adhesion molecules, including CCL19/CCL21 (CCR7 axis), CXCL13 (CXCR5 axis), and VCAM-1, ICAM-1, and MAdCAM-1. These cues drive B-cell and $CXCR5^+$ Tfh positioning toward follicle-like areas, and $CCR7^+$ T cells and DCs toward T-zone–like regions, thereby supporting antigen presentation and T-cell priming.[9,28] This molecular network is among the most conserved organizer–chemokine switches in lymphoid organogenesis.[9,16] In oncology, CXCL13 and CCL19/CCL21 are also frequent components of TLS-associated transcriptomic signatures used to infer TLS presence or immunotherapy benefit.[3,29,30] Unlike encapsulated SLOs with well-defined sinus and lymphatic structures, TLS are usually not encapsulated and may have incomplete sinus. Their maturation depends more on local stromal scaffolds and ongoing cell entry through HEVs. When stimulation weakens, TLS can regress or return to earlier aggregates, highlighting their plasticity and the fact that TLS engineering depends strongly on tissue context.[10,31]

At the vascularization stage, HEV provide a continuous gateway for lymphocyte entry into TLS. HEV endothelium expresses L-selectin ligands (commonly marked by PNAd/MECA-79 in tumors) and presents chemokines (e.g., CCL21) and adhesion molecules (ICAM-1/VCAM-1), enabling rolling, firm adhesion, and transendothelial migration of circulating lymphocytes and thereby sustaining recruitment of $CCR7^+$ naïve/central-memory T cells and subsets of B cells.[32,33] Tumor-associated HEVs are thought to form through a program similar to that in SLOs. A key driver is $LT\alpha_1\beta_2$ to LTβR signaling through the non-canonical NF-κB pathway. $LT\alpha_1\beta_2^+$ inducer-like cells bind LTβR on endothelial or stromal cells, activate PNAd-related glycosylation, and increase adhesion molecules and chemokines, which promotes HEV-like changes and sustained lymphocyte entry.[33] LIGHT can promote TLS recruitment programs across models and, when targeted to tumor vasculature, has been coupled to intratumoral TLS induction.[33,34] Inflammatory cues such as TNF-α, IL-1β, and type I/II interferons can enhance endothelial responsiveness to LTβR signaling and amplify recruitment programs, thereby lowering the threshold for HEV formation.[33] HEV emergence typically parallels the establishment of stromal networks and homeostatic chemokine axes and correlates with TLS maturation and lymphocyte flux.[33] Notably, endothelial Rbpj conditional deletion can bias endothelium toward an HEV-like phenotype and induce spontaneous TLS across multiple organs, suggesting a restraining role for Notch–Rbpj signaling in maintaining vascular identity and limiting TLS initiation.[35]

The formation and maintenance of a follicular dendritic cell (FDC)-like network is often seen as a key turning point. It marks the shift from simple "structural clustering" to "functional follicle formation." FDCs can capture and hold complement-tagged immune complexes through complement receptors (e.g., CR1/CR2) and Fc receptors. This allows them to present antigens in their native form for a long time and build an "antigen reservoir" that B cells can sample repeatedly. This converts transient, diffuse antigen exposure into a sustained platform for affinity selection.[36,37] On this basis, Tfh cells support germinal-center (GC) reactions through CD40L–CD40 interactions and a permissive cytokine milieu that facilitates class-switch recombination (CSR). IL-21, among other helper cytokines, promotes GC B-cell proliferation and survival and sustains GC programs, thereby enhancing affinity maturation. This coordinated Tfh and B-cell circuit increases activation-induced cytidine deaminase (AID) expression and drives AID-dependent somatic hypermutation (SHM) and class-switch recombination (CSR). It ultimately produces memory B cells and plasma-cell or antibody lineages with higher affinity and more specialized functions.[38] Collectively, LTi/LTo signaling, chemokine-driven lymphocyte recruitment, and HEV-supported trafficking coordinate a stepwise maturation of TA-TLS from early aggregates to germinal center–like structures (Figure 1).

TLS CLASSIFICATION

Because TLS can be seen by morphology but are functionally flexible, structures labeled as "TLS" can differ greatly in maturation stage, spatial location, and cellular-state composition. Consequently, the direction and strength of associations between TLS and prognosis or therapeutic response are not necessarily uniform. There is currently no single, universally adopted TLS classification framework. Instead, studies commonly classify TLS using several dimensions that may overlap, such as maturation, spatial localization, cellular composition, developmental trajectories, and molecular signatures or quantitative scores. Many studies also combine these dimensions to improve comparisons across cohorts and to reduce the information loss that comes from simply reporting TLS-positive or TLS-negative results.[3,39]

Classification by maturation / histological organization

Maturation is the most commonly used way to classify TLS, and it is also relatively easy to replicate across different cohorts. It directly shows whether a TLS has formed separate B- and T-cell areas, built an FDC network, and started a GC reaction. This goes beyond simply noting lymphoid aggregates, and serves as an indicator of the ability to generate strong adaptive immune responses.[40,41]

On routine hematoxylin-and-eosin (H&E) sections, TLS usually appear as

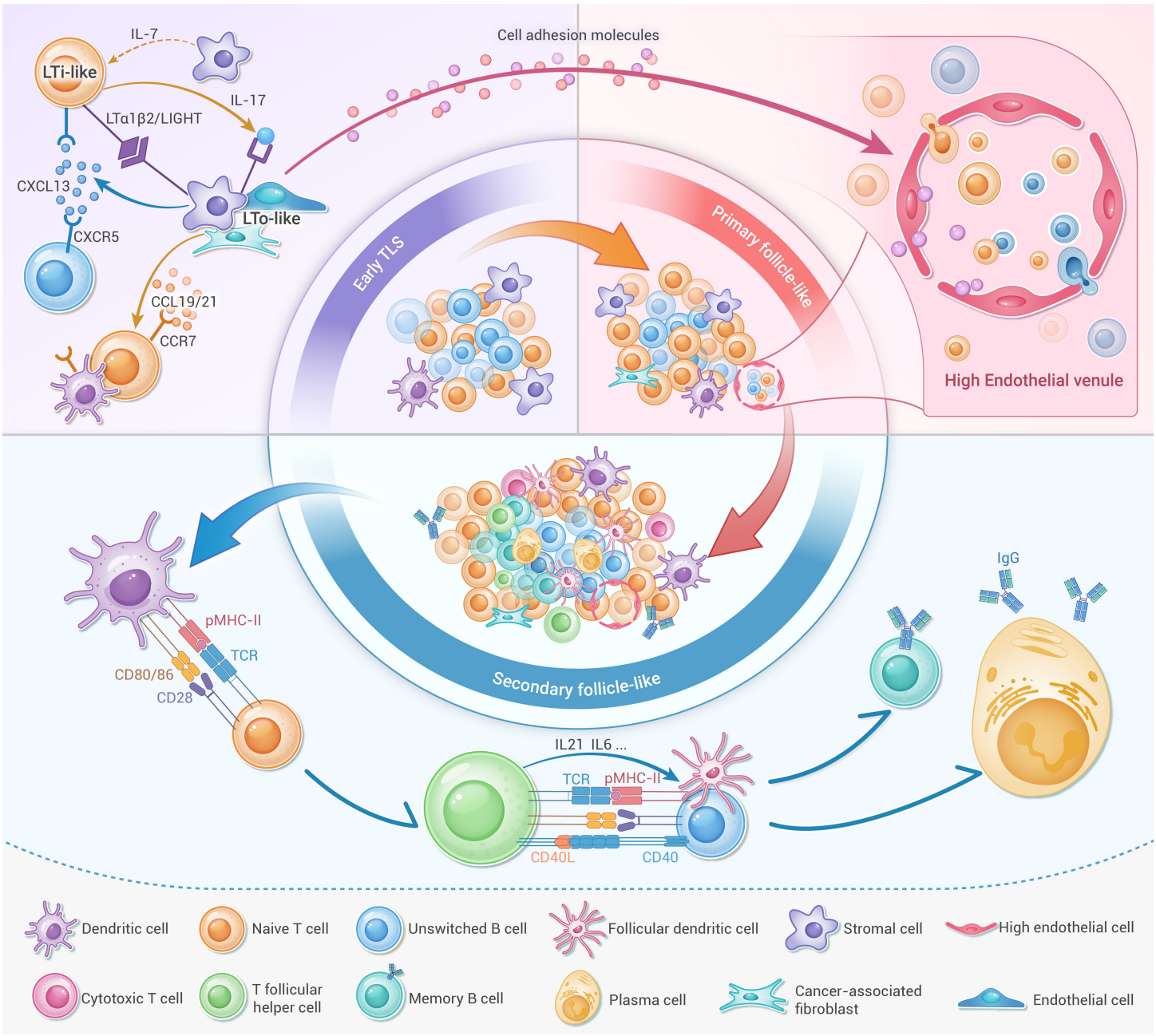

Figure 1. Initiation, formation, and maturation of tumor-associated tertiary lymphoid structures (TA-TLSs) LTi-like signals, including LTα1β2/LIGHT, engage LTo-like stromal cells and promote lymphoid-organizing programs associated with induction of adhesion molecules and homeostatic chemokines, including CXCL13 and CCL19/CCL21, thereby recruiting CXCR5$^+$ B cells and CCR7$^+$ T cells/dendritic cells to nascent aggregates. IL-17 and stromal-derived IL-7 may further support this feed-forward process. Concurrently, formation of high endothelial venules facilitates lymphocyte entry and supports progressive maturation from early TLSs to primary follicle-like and secondary follicle-like TLSs. In more mature TLSs, follicular dendritic cells and T follicular helper cells help sustain germinal center-like reactions through CD40L-CD40 interactions and cytokine support, including IL-21 and IL-6, thereby promoting B-cell maturation and differentiation into memory B cells and plasma cells.

dense lymphocyte aggregates. Immature structures often have indistinct borders and mixed cellular contents, whereas mature TLS can form round or ovoid nodules with evolving mantle-like layering and a paler central zone suggestive of GC-like activity.[3,42] H&E is sensitive for finding aggregates, but it cannot reliably show features that define TLS maturation. Therefore, a common pathology workflow uses three steps: first H&E screening, then immunohistochemistry (IHC) for confirmation and staging, and when needed, multiplex immunofluorescence or multiplex IHC (mIF/mIHC) for more detailed cell typing. A basic IHC panel usually includes CD3 and CD20 to define T- and B-cell zones, and CD21 or CD35 to identify FDC networks. CD23, BCL6, AID, and Ki-67 are used to indicate GC-related programs, and PNAd (MECA-79) is used to mark HEVs. In some clinical cohorts, MECA-79$^+$ HEV density has been used as an objective measure of TLS burden and has been linked to treatment response and/or prognosis.[43] DC-LAMP can assist in identifying mature DC aggregates.[44,45] A three-level scheme has been widely used across tumor types[10,46–49]: early TLS (E-TLS), primary follicle-like TLS (PFL-TLS), and secondary follicle-like TLS (SFL-TLS). This scheme often uses CD21 and CD23, assessed by double staining or serial sections, as key staging markers. E-TLS are dense aggregates without CD21$^+$ FDC networks or CD23$^+$ GC signals. PFL-TLS show follicle-like structures with a B-cell core, a surrounding T-cell ring, and a CD21$^+$ FDC network, but they still lack CD23$^+$ GC. SFL-TLS add CD23$^+$ GC areas on top of the PFL structure, which matches the paler GC-like core seen on H&E.[42]

E-TLS are closer to "inflammatory aggregates." T and B cells are mixed together, and antigen presentation and T-cell priming can still occur. However, because there is no stable follicle or GC scaffold, long-term production of high-affinity antibodies and memory B cells is limited. In some tumor contexts, this stage may also be more vulnerable to enrichment of Tregs and suppressive myeloid elements, leading to structurally present yet functionally inefficient.[3,50] A key transition in PFL-TLS is the emergence of an

FDC network. CD21/CD35$^+$ FDCs suggest that antigen and immune-complex capture via complement receptors have started. This provides longer antigen exposure and stronger selection pressure for B cells, and it allows more frequent helper interactions with Tfh or peripheral helper T cells (Tph) at the B and T cell interface.[40,50] However, without a CD23$^+$ GC program, somatic hypermutation, selection, and class switching may be incomplete; functional outputs may skew toward organization and initiation, and progression toward a mature GC depends on the local strength of cues such as IL-21 and CD40L.[22,51] SFL-TLS (GC$^+$ TLS) indicate that TLS have gained lymph-node-like capacity for humoral immune responses. CD23$^+$ areas often overlap with BCL6$^+$ B cells, highly proliferative Ki-67$^+$ B cells, and AID-related programs. In some cases, they also show dark-zone and light-zone-like layering, although this pattern is not always typical in tumors. These features support ongoing somatic hypermutation and affinity selection, and they are consistent with the generation of memory B cells and plasma cells. Across multiple tumor cohorts, GC$^+$ TLS show more stable associations with stronger antigen-specific humoral immunity and a higher probability of response to ICB.[29,30,52]

For research and translational assessment, mIF/mIHC can further resolve functional heterogeneity by jointly reading out Tfh/Tfr modules (e.g., PD-1, CXCR5, ICOS, FOXP3), B-cell differentiation spectra (naïve/memory/plasma), DC maturation states, and inhibitory axes (e.g., PD-L1, IDO1). Quantitative features such as B/T segregation, GC cell density, and the fraction of suppressive components can then align 'morphological maturation' with 'immunological activity or suppression' within the same spatial framework, reducing observer variability.[41,50]

Classification by spatial localization

This framework commonly distinguishes intratumoral TLS (iTLS) from peritumoral TLS (pTLS) and may further subdivide by tumor parenchyma, stroma, and invasive margin. TLS formation depends on local vascular and stromal structure, chemokine gradients, and immune entry routes. These factors differ between intratumoral and peritumoral regions. If TLS positivity is reported without spatial information, real biological differences may be hidden, and links to clinical outcomes or treatment effects may become less consistent.

pTLS do not necessarily carry the same immunological implications as iTLS.[53,54] This issue is especially important in tumors that develop with chronic inflammation, such as hepatocellular carcinoma (HCC). Several studies in HCC have assessed iTLS and pTLS separately, suggesting that their clinical associations and local immune states do not always match,[55–59]iTLS were associated with a reduced risk of early recurrence.[57,60,61] By contrast, the prognostic direction of pTLS appears more contingent on operational spatial boundaries and the underlying chronic inflammatory context. For example, Zhang et al. defined peritumor tissue as liver parenchyma within 1 cm of the tumor margin and found that pTLS were associated with neutrophil infiltration and worse outcomes. This suggests that, under this definition, pTLS may reflect an immune environment shaped by chronic inflammation and biased toward myeloid cells.[58] Earlier mechanistic work also proposed that hepatic ectopic lymphoid-like structures (ELSs) formed during inflammation could create a niche that supports tumor progenitor cells, and this was linked to worse prognosis.[59]Conversely, retrospective cohort in HCC[55,56] reported that higher pTLS (with peritumor defined as a 5-mm ring beyond the invasive margin) density was associated with better overall survival (OS) . These observations suggest that even within the category of "pTLS," prognostic direction may shift substantially with the spatial window and the treatment context of the cohort.

Notably, some studies combine spatial location with maturation staging (E-TLS/PFL-TLS/SFL-TLS). They suggest that differences in prognosis and immunotherapy effects across locations may relate to maturation distributions.[62–64] In clear cell renal cell carcinoma (ccRCC), TLS were classified as tumor-proximal TLS (within the invasive margin) or tumor-distal TLS (in normal tissue more than 10 mm from the invasive margin). Tumor-distal TLS were enriched for E-TLS, whereas tumor-proximal TLS were enriched for SFL-TLS. The presence of tumor-proximal TLS was associated with longer OS and progression-free survival (PFS), whereas the presence of only tumor-distal TLS was associated with shorter OS and PFS.[63,65] In a cohort of small-intestinal adenocarcinoma (jejunum/ileum), TLS were assigned to intratumoral (IT), invasive margin (IM), and peritumoral (PT) locations. Spatially, TLS were more frequently observed at the invasive margin and peritumoral regions; IT-TLS were less common and tended to be less mature. Regarding maturation differences, IT-TLS more often showed an E-TLS phenotype (P=0.007). SFL-TLS were more likely to appear at the invasive margin (P=0.032) and tended to be more common in peritumoral regions (P=0.057).[66]

At present, the spatial boundaries used for peritumoral TLS (pTLS) and intratumoral TLS (iTLS) are not standardized across studies or tumor types, which limits comparisons between cohorts. In practice, "peritumoral" is most often defined as about 0.5 to 10 mm beyond the invasive margin or tumor boundary,[48,58,67–69], but the exact cutoff varies. (Table 1). In some studies, no clear cut-off values were reported to define iTLS and pTLS, but rather based on pathological regional partition[54,66,70] or whole-slide image (WSI) partition.[71,72]

Classification by cellular composition and immune activity

As spatial transcriptomic/proteomic profiling and high-throughput multiplex immune imaging are increasingly used, several studies suggest that TLS stratification does not need to depend only on "canonical GC-like morphology," and can instead be based on the cellular composition and immune-activity programs within TLS region of interests (ROIs) and the surrounding microenvironment. In a spatial multi-omics investigation of adult-type diffuse gliomas (n = 642), TLS were detected in about 15% of tumors, and their presence was linked to perivascular spatial remodeling and reshaping of extracellular-matrix components. The authors further classified TLS into three categories, T-low-TLS, B:T-TLS, and PC-TLS, based on differences in cellular composition and immune activity. Notably, all subtypes lacked a classical GC architecture, yet a subset of TLS still exhibited evidence of dynamic adaptive immune function. Concretely, T-low-TLS reflected a T-cell-depleted, myeloid-enriched immune state. B:T-TLS showed B and T cell co-localization and higher activity in programs linked to antigen presentation and dendritic cell and T cell interaction; this subtype also more often contained mature DC states (e.g., LAMP3$^+$ DCs), suggesting stronger local antigen presentation and T-cell activation. PC-TLS showed stronger plasma-cell differentiation and antibody-production signatures, including IgA$^+$/IgG$^+$ plasma-cell generation and higher expression of immunoglobulin transcripts and plasma-cell markers (e.g., DERL3 and TENT5C). Glioma is typically viewed as an immunologically "cold" tumor. Even so, TLS-associated functional adaptive immune responses were observed in a subset of patients. Importantly, TLS stratification using a "composition–activity/function spectrum" correlated with survival. Therefore, this scheme may support more detailed, mechanism-based interpretation and help guide therapeutic stratification.[73]

Classification by developmental trajectories

Trajectory-based frameworks interpret TLS heterogeneity as the outcome of distinct maturation trajectories. TLS categorized as "immature" may progress along a maturation trajectory or, under tumor-microenvironmental pressures, deviate from such a trajectory, leading to divergent subsequent structural features and immune outputs. In a near single-cell spatial transcriptomics study of HCC, immature TLS were further partitioned by trajectory inference into conforming TLS and deviating TLS. Conforming TLS exhibited B-cell differentiation trajectories highly concordant with those of mature TLS in trajectory analyses, with continuous expression gradients of gene modules such as CXCL13 and AID across mature and conforming TLS. Histologically, conforming TLS could display relatively clear T/B segregation and follicularization trends despite lacking a canonical GC. Functionally, conforming TLS, although not fully mature morphologically, were proposed to harbor niche functions linked to anti-PD-1 response. In contrast, deviating TLS showed stalled B-cell differentiation and impaired HEV development, which may promote a more immunosuppressive microenvironment. Importantly, "trajectory-based" subtyping relies on spatial-omics datasets that are fine-grained enough to distinguish cellular states and their spatial neighborhoods. With lower-resolution data or datasets with limited marker dimensionality, the stability and reproducibility of such inferences decrease substantially. Thus, this framework should be regarded as a "high-resolution interpretive tool" for TLS heterogeneity rather than a universally applicable morphologic classification standard.[74]

Table 1. Spatial definitions of tumor-associated tertiary lymphoid structures (TLS) and clinical correlations across cancer types.

Cancer type	Sample size (N)	Spatial definition	TLS detection method	Prognostic correlation	Reference
Breast Cancer	167	pTLS: ≤5 mm outside invasive margin	H&E + IHC	pTLS positivity or higher density: DFS↓, OS↓	[53]
Breast Cancer	95	pTLS: peritumoral region (no distance cut-off reported)	IHC + mIF	High pTLS density: OS↑, DFS↑	[54]
CCA	571	WSI partition: intratumor (T) vs peritumor (P)	H&E + IHC	Higher T-score (iTLS-high): OS↑; higher P-score (pTLS-high): OS↓	[72]
ccRCC	395	Tumor-proximal: invasive margin; Tumor-distal: normal tissue >10 mm from invasive margin	IHC + mIF	Tumor-proximal TLS+: OS↑, PFS↑; tumor-distal TLS+: OS↓, PFS↓	[65]
ccRCC	659	Intra-TLS: invasive margin; peri-TLS: normal tissue >10 mm from invasive margin	IHC + mIF + ST	Intra-TLS and SFL-TLS: OS↑	[63]
CRC	109	pTLS: ≤7 mm outside tumor front	IHC	High SFL-TLS: 3-year recurrence↓; low maturity: recurrence↑	[48]
CRLM	178	pTLS: ≤2 mm from tumor boundary	IHC + bulk RNA-seq + scRNA-seq + scBCR-seq + ST	TLS+ (iTLS+pTLS): OS↑, RFS↑	[25]
CRLM	603	WSI partition: intratumor (T score) vs peritumor (P score)	IHC	High T score: RFS↑, OS↑; high P score: RFS↓, OS↓	[71]
ESCC	350	pTLS: ≤1000 μm outside tumor nest boundary	H&E + IHC	Higher pTLS density: OS↑	[42]
gastric cancer	59	Regions: tumor core (TC), invasive margin (IM; ~500 μm centered on boundary), adjacent normal (N)	H&E + IHC + scRNA-seq + ST	TC-TLS+: irOS↑	[172]
HCC	170	iTLS: intratumoral tumor region; pTLS: peritumoral tissue 1 cm from tumor edge (tumor-free)	H&E + IHC + 12-Chemokines signatures	pTLS+ : OS↓, DFS↓; iTLS+: DFS↑	[58]
HCC	170	iTLS: intratumoral tumor tissue; pTLS: peritumoral liver parenchyma 5 mm from infiltrative border	H&E + IHC	High pTLS density: OS↑, RFS↑; iTLS+: RFS↑;	[55]
HCC	701	pTLS: peritumoral liver parenchyma 5 mm from invasive tumor border	IHC	Higher pTLS density: OS↑, RFS↑	[56]
HCC	71	iTLS and pTLS; no unified mm distance cut-off reported	H&E + IHC + bulk RNA-seq	Post-treatment iTLS high: RFS↑; pTLS: NS	[70]
HCC	273	non-tumoral liver TLS: non-tumoral regions <2 mm from the tumor border	H&ES + IHC	iTLS+: early recurrence↓; higher TLS maturity: recurrence↓; non-tumoral liver TLS: NS	[60]
HCC-LT	666	TLS scores (0–3) for intratumoral (iTLS) and peritumoral (pTLS) regions were evaluated	RNA-seq + scRNA-seq	High iTLS score: OS↑, RFS↑; iTLS absent: OS↓	[61]
iCCA	962	pTLS:normal tissue located 5 mm away from the tumor edge	IHC	High tumor TLS (T-TLS): OS↑; high peritumor TLS (P-TLS): OS↓	[68]
NSCLC	82	IT-TLS (intratumoral), IM-TLS (invasive margin), and PT-TLS (peritumoral) IM defined as 500 μm on both sides of the tumor–normal lung boundary	IHC	High IM E-TLS density: OS↓, PFS↓	[62]
NSCLC	536	Intratumoral: the tumor boundary; periphery: non-tumoral tissue 2 mm outside the invasive margin;	IHC	High total TLS (especially peripheral): OS↑; intratumoral TLS: NS	[69]
Primary adenocarcinoma of jejunum and ileum	54	IT-TLS (intratumoral), IM-TLS (invasive margin), and PT-TLS (peritumoral)	H&E + IHC	Higher SFL-TLS: DFS↑; higher PT-TLS : OS↑	[66]

Abbreviations: TLS, tertiary lymphoid structure; iTLS, intratumoral TLS; pTLS, peritumoral TLS; TC, tumor core; IM, invasive margin; WSI, whole-slide image; H&E, hematoxylin and eosin; HES, hematoxylin–eosin–saffron; IHC, immunohistochemistry; mIF, multiplex immunofluorescence; ST, spatial transcriptomics; bulk RNA-seq, bulk RNA sequencing; scRNA-seq, single-cell RNA sequencing; scBCR-seq, single-cell B-cell receptor sequencing; OS, overall survival; PFS, progression-free survival; DFS, disease-free survival; RFS, recurrence-free survival; ORR, objective response rate; pCR, pathologic complete response; MPR, major pathologic response; GC, germinal center; TME, tumor microenvironment; Tfh, T follicular helper cell; Treg, regulatory T cell; ccRCC, clear cell renal cell carcinoma; CRC, colorectal cancer; CRLM, colorectal liver metastases; ESCC, esophageal squamous cell carcinoma; HCC, hepatocellular carcinoma; HCC-LT, HCC after liver transplantation; iCCA, intrahepatic cholangiocarcinoma; CCA, cholangiocarcinoma; NSCLC, non-small cell lung cancer; irOS, immune-related overall survival; NS,not significant

Taken together, current TLS classification frameworks can be understood along four partially overlapping axes: maturation, spatial localization, functional composition, and developmental trajectory. Among these, maturation remains the most broadly reproducible pathology-based framework, whereas spatial localization helps explain why TLS with similar morphology may associate with different clinical outcomes. Composition- and trajectory-based frameworks further refine TLS heterogeneity by capturing immune activity states and lineage progression that may not be apparent from morphology alone. Therefore, rather than treating TLS as a binary feature, future studies should ideally integrate these dimensions to improve biological interpretation and cross-cohort comparability.

TLS-MEDIATED TUMOR IMMUNE MECHANISMS

Framing antitumor immunity as an integrated process, Chen and Mellman introduced the canonical "cancer-immunity cycle," outlining a series of steps encompassing tumor antigen release, antigen presentation, T-cell activation/expansion, effector T-cell homing and infiltration, and tumor-cell killing.[2]

However, in solid tumors, this cycle is often blocked by an immunosuppressive tumor microenvironment (TME). In particular, tumor signal-driven remodeling of tumor-draining lymph nodes (tdLNs) and suppression of antigen presentation and priming can weaken the priming step.[75,76] Meanwhile, activated T-cell migration and entry into tumors are limited by multiple structural and molecular barriers.[77] For example, stromal-associated galectin-1 can selectively prevent immunogenic DCs from moving through the ECM and crossing lymphatic endothelium. This reduces the number of migratory DCs reaching draining lymph nodes and lowers the quality of antitumor immune priming.[78] In addition, abnormal tumor vessels and hypoxia can together create an immune-excluded setting. Together with the immunomodulatory effects of the VEGF pathway, they limit effective effector T-cell homing and tumor entry.[77,79,80]

In this context, tumor-associated tertiary lymphoid structures (TA-TLSs) are often viewed as "antitumor amplifiers," mainly because they can organize local clusters of antigen-presenting cells and T and B cell interaction networks within tumors. This makes local responses more like an in situ adaptive immune microenvironment.[3,81] When TA-TLS becomes more mature and show GC-like reactions, they are more likely to support B-cell affinity maturation and plasma-cell differentiation. With Tfh-like help, these processes can further boost responses and strengthen sustained effector output.[3,10] Meanwhile, TA-TLS often co-occurs with high endothelial venules (HEVs), which can serve as entry portals for lymphocyte extravasation into tumors , providing a sustained cellular supply for local responses.[82] Importantly, TA-TLSs are not homogeneous "lymphocyte aggregates". They are highly heterogeneous in cellular composition, maturation, and functional output and are continuously remodeled across time and space.[3,6,10]

T cells

Follicular helper T (Tfh) cells, typically marked by CXCR5, PD-1, ICOS, and BCL6, are key regulators of B-cell activation and GC-like reactions in TLS. They are commonly enriched in the B-cell follicle/GC-like compartment and at the B–T interface of TLS.[83,84] Through contact-dependent CD40L-CD40 signaling and helper cytokines such as IL-21 and IL-6, Tfh cells promote B-cell proliferation, differentiation, and class-switch recombination. This supports the generation of memory B cells and plasma cells.[85–87] In TLS that develop mature GC-like architecture, Tfh cells cooperate with follicular dendritic cell (FDC) networks to shape the post–somatic hypermutation selection microenvironment, facilitating affinity maturation and higher-affinity antibody responses.[85,87,88] The Tfh–B axis in mature TLS is therefore coupled to adaptive immune outputs, including humoral effector functions and immune memory. These outputs may also shape local antigen presentation and indirectly affect the strength and persistence of cytotoxic responses. However, these effects depend strongly on TLS maturation and on counter-regulatory circuits such as Tfr and Treg modules.[84,86,88] Besides canonical Tfh cells, studies have reported PD-1^{hi} CXCR5− CXCL13^{+} CD4^{+} B-helper subsets with Tph/Th-CXCL13-like features in TLSs across breast cancer[89], ovarian cancer[90], and nasopharyngeal carcinoma.[91] These cells may increase recruitment of CXCR5^{+} B cells into TLSs through the CXCL13 to CXCR5 pathway.[89–91]

Precursor exhausted-like CD8^{+}T cells (Tpex) are frequently enriched in the T-cell zone, dendritic cell (DC)-rich areas, and the B–T interface of mature TLS. Spatial and single-cell studies in non-small cell lung cancer (NSCLC),[92] esophageal cancer,[93] head and neck squamous cell carcinoma,[83] and colorectal cancer[94] indicates that PD-1^{+}TCF1^{+}TCF7^{+} Tpex tend to reside in intratumoral or peritumoral TLSs, or in TLS-like lymphoid aggregates. This supports the idea that TLSs provide a niche that maintains these cells and supports their renewal. This population typically expresses stem-like or maintenance genes (TCF7/TCF1, LEF1, and IL7R/CD127), often with intermediate rather than very high PD-1 levels. It also shows relatively low levels of terminal cytotoxic molecules such as GZMB、PRF1. In some tumors, CXCR5 or other chemokine receptors linked to follicle homing are also observed.[95–97] With sustained antigen presentation and co-stimulatory support from mature DCs, Tpex cells can differentiate locally into effector cytotoxic CD8 T cells. These cells often increase NKG7, GZMB, PRF1, and IFNG, and then move into tumor tissue to kill tumor cells.[96–98] The capacity of TLS to maintain a TCF1^{+} PD-1^{+} CD8^{+} T-cell niche appears to depend on TLS maturation. In one high-grade serous ovarian cancer (HGSOC) study, mature TLS (mTLS) were uncommon (~16% of cases), and the broader tumor microenvironment (TME) was dominated by TIM3^{+} PD-1^{+} CD8^{+} T cells. The authors suggested that insufficient TLS maturation may limit maintenance of the more "immune checkpoint inhibitors (ICI)-sensitive" TCF1^{+}PD-1^{+} CD8^{+} niche. This could shift the balance toward "ICI-insensitive" TIM3^{+}PD-1^{+} lineages and may help explain the relatively low response rates to standard ICIs in HGSOC.[99]

Treg cells (e.g., FOXP3, IL2RA/CD25, and CTLA-4) are commonly located in the T-cell zone and in proximity to DC-rich regions within TLS. They may expand from thymus-derived Tregs or arise via induction in the TME. Their suppressive mechanisms include dampening DC co-stimulation, constraining effector T-cell proliferation, and reshaping local activation thresholds through cytokine and metabolic competition. In a murine lung adenocarcinoma model, Tregs within tumor-associated TLS (TA-TLS) suppressed antitumor T-cell responses. Depleting Tregs increased co-stimulatory molecule expression on DCs in TA-TLSs and boosted T-cell proliferation.[100] In a retrospective cohort of resectable NSCLC (n=338), IHC and multiplex IF showed that Tregs were mainly in the stroma, with some entering TLSs. A combined grouping based on TLS-mature DCs (DC-LAMP^{+}), CD8^{+} T cells, and TLS Treg density improved risk separation. The "TLS-Treg^{High} + TLS-DC^{Low} + CD8^{Low}" group had the poorest OS.[101] In breast cancer TLS, follicular regulatory T (Tfr) cells (CD25^{+} CXCR5^{+} GARP^{+} FOXP3^{+}) have been identified as a functional Treg subset. Tfr cells can bind latency-associated peptide (LAP)-bound TGF-β through glycoprotein A repetitions predominant (GARP) and, with the help of integrins, activate TGF-β locally at the immune synapse to suppress Tfh-driven B cell and GC reactions. Neutralizing TGF-β reduces this Tfr-mediated suppression of Tfh function. This supports an opposing circuit in TLSs between "Tfh-driven humoral and GC responses" and "Tfr (GARP-TGF-β)-mediated inhibition of Tfh." [89]

B cells

The B-cell lineage is the most direct cellular substrate linking TLS 'structural maturation' to 'humoral effector output,' and functional layering is usually tightly coupled to spatial positioning. Within follicular/GC compartments, GC B cells with proliferative and somatic hypermutation programs can be observed (e.g., AID, BCL6, and Ki-67 signatures). Outside follicles and in the tumor stroma, memory B cells and plasma cells are commonly found. With TLS maturation, clonally trackable B-cell receptor (BCR) expansion and antibody-lineage evolution can be detected. In tumor TLS, IgG is frequently the predominant isotype, followed by IgA, whereas IgM is more often observed in earlier-stage or less mature lymphoid aggregates.[5,6]

At the Fc end, IgG4 has weaker canonical effector functions than IgG1 or IgG3. IgG4 can undergo Fab-arm exchange (FAE) in vivo, which produces bispecific antibodies that act like single-binding antibodies and reduce immune-complex formation and crosslinking effects.[102] Multiple studies in esophageal squamous cell carcinoma (ESCC) have reported that high IgG4 expression within TLS is associated with poor prognosis.[103,104] In an ESCC study, enrichment of IgG4^{+} cells in TLS negatively correlated with CD8^{+} T-cell density in mature TLS. Patients also showed elevated serum IgG4 and IL-10 levels with a positive correlation. In vitro, IgG4 promoted monocyte polariza-

tion toward M2-like macrophages. Based on these results, the authors proposed that an IgG4 and IL-10 axis may increase local immunosuppression by promoting M2 polarization within TLSs. They also suggested this axis as a possible therapeutic target.[103]

TLS with distinct B-cell compositions and activation states may diverge functionally toward either immunosuppressive phenotypes or antigen-driven protective immune reactions. In melanoma metastases (n = 64), Lynch et al. reported that a lower fraction of CD21$^+$ B cells within TLS was associated with longer OS (OS), whereas a lower fraction of AID$^+$ B cells was associated with shorter OS.[49] Chen et al. further reported that IGLL5$^+$ B cells, in multiple models and human samples, could bind LTβR on HEVs and alter LTβR structure, which suppresses non-canonical NF-κB signaling. This lowers several adhesion molecules and chemokines, leading to HEV defects and TLS breakdown. In diverse models, including patient-derived xenografts (PDX), targeting this axis helped maintain or restore TLS homeostasis and improved immunotherapy responses.[105] Multi-omics analyses have also delineated plasma-cell heterogeneity in TLS-associated compartments. In cervical cancer, Huang et al. grouped plasma cells into different transcriptional states. MANF_PC was enriched in normal tissue, showed stronger antibody synthesis and secretion features, and was linked to better prognosis. In contrast, HSPA1B_PC was enriched in tumor tissue, was linked to worse outcomes, and was spatially associated with TLS signals. Spatial transcriptomics and multiplex IF suggested significant co-localization of HSPA1B_PC with immunosuppressive T-cell subsets (Treg and Th17) within TLS. This subset also expressed higher levels of several immune regulatory factors (e.g., TGFB3, IL1B, and TNFSF13B) than MANF_PC. The authors therefore proposed that HSPA1B_PC may relate to an 'immunosuppressive TLS microdomain' and represent a candidate interventional target, while emphasizing that causal roles require functional validation.[106]

The cellular origin of tumor-associated plasma cells (PCs) remains unresolved. Existing evidence has largely followed two non-mutually exclusive lines. One line supports a continuous in situ process within intratumoral TLS, from B-cell activation through high-frequency somatic hypermutation (SHM) and class-switch recombination (CSR) to plasma-cell differentiation. For example, in renal cell carcinoma, spatial transcriptomic and histopathological evidence suggested that TLS can 'generate and disseminate' antitumor antibody-secreting plasma cells. IgG$^+$/IgA$^+$ plasma cells co-localized with TLS and extended along stromal trajectories toward the tumor bed, and IgG coating of tumor cells was observed.[107] Another model suggests that peripheral lymphoid organs, including tumor-draining lymph nodes (TDLNs), can contribute importantly to B-cell clonal diversification and expansion. In pancreatic ductal adenocarcinoma (PDAC), one study reported continuity between the local tumor B-cell repertoire and SLOs.[108] In addition, evidence from lung cancer indicates that tumor-draining lymph nodes can influence the maturation of intratumoral TLSs, supporting the idea that local and peripheral humoral immune niches may be functionally coupled rather than strictly separated.[109] Tumor-specific observations further suggest that plasma cells may also accumulate and function outside a TLS-centered context. In glioblastoma (GBM), a CCL2–CCR2 axis was proposed to drive plasma-cell infiltration into the tumor microenvironment, including glioma stem cell (GSC)-associated niches. In this setting, plasma-cell-derived IgG was implicated in sustaining glioblastoma stem-cell properties.[110] Overall, one simple interpretation is that when mature TLSs are present inside tumors, remain structurally intact, receive cells through HEVs, and support GC programs, local plasma-cell generation and later exit may become a major source. This can create a humoral effector front near the tumor bed.[107] Conversely, when TLSs are rare, immature, or strongly suppressive and GC programs are limited, draining lymph nodes or peripheral SLOs may play the main role in clonal expansion and affinity maturation. Clones can then traffic and home back to the tumor to supply it.[111,112] This model remains to be tested with further experimental validation.

Myeloid cells

Within TLSs, dendritic cells (DCs) comprise several functionally distinct subsets. These include conventional type 1 DCs (cDC1s), which are efficient at cross-presenting antigen to CD8+ T cells, and conventional type 2 DCs (cDC2s), which more commonly support CD4+ T-cell priming and immune coordination. In addition, tumors can contain mature regulatory DCs (mregDCs), a transcriptionally distinct activated DC state characterized by both migration and immunoregulation associated programs. Monocyte-derived DCs or transitional populations such as DC3 may also be present.[83] Early studies in primary lung tumor cohorts suggested that a high density of DC-LAMP$^+$ mature DCs within TLSs was independently associated with longer survival. It also improved risk stratification among patients with high CD8$^+$ T-cell infiltration, suggesting that TLSs enriched in mature DCs may strengthen the protective effects of CD8$^+$ T cells.[113] In head and neck squamous cell carcinoma, cDC2 showed the greatest number of significant interaction pairs within TLS-associated cellular clusters. It also showed key co-stimulatory axes in mature TLSs, such as TNFSF13B to TNFRSF13C or TNFRSF17. Meanwhile, LAMP3$^+$ mregDCs exhibited communication potential spanning migratory maturation and immune regulation, with expression of molecules including CCL22/CCL17, CCL19, CD80/CD86, IL12B/IL15, and PD-L1/PD-L2.[83] Importantly, when DC-LAMP is used as a mature-DC marker in clinical histology, tissue-specific confounding can occur. For example, in lung tissue, type II alveolar epithelial cells may also stain positive for DC-LAMP. Thus, in lung cancer specimens, quantification based on DC-LAMP alone may be biased and is better supported by morphology, co-localization criteria, or multi-marker validation.[114]

Under certain therapeutic pressures or tumor-derived cues, a fraction of LAMP3$^+$ DCs may also shift toward immunoregulatory programs, thereby exerting suppressive effects on TLS formation and function. In a study of microsatellite-stable (MSS) rectal cancer treated with neoadjuvant chemoradiotherapy (NCT), Wang et al. hypothesized that LAMP3$^+$ IRF8$^+$ DCs could suppress TLS formation by promoting Tfh exhaustion. Their marker genes were positively correlated with exhaustion signatures and negatively correlated with TLS signatures. It also suggested higher activity of the IRF8 regulon in non-responders, and the IRF8 regulon negatively correlated with TLS formation while positively correlating with immunosuppressive capacity. A retrospective histological cohort further showed a significant inverse association between CD11c$^+$ LAMP3$^+$ IRF8$^+$ DCs and TLS density.[115]

Myeloid-derived suppressor cells (MDSCs) tend to accumulate in functionally less mature TLSs, such as TLSs without stable GC-like reactions or TLSs resembling primary follicle-like structures. They are especially common in T-zone or myeloid-rich areas, and they are often linked to weak effector T-cell activation or a lack of tumor-specific responses.[10,116] Both polymorphonuclear MDSCs (PMN-MDSCs) and monocytic MDSCs (M-MDSCs) can be observed in TLS.[116] PMN-MDSCs frequently display CD15$^+$/LOX-1 (OLR1)$^+$ phenotypes and can express high arginase-1 (ARG1),[117] whereas M-MDSCs often display CD14$^+$ phenotypes with inflammatory–suppressive programs such as S100A8/S100A9.[118] Their recruitment commonly involves the CCL2–CCR2 axis.[119] Both subsets can upregulate PD-L1 (CD274) and suppress T-cell signaling through reactive oxygen species(ROS) or reactive nitrogen species (RNS) -mediated oxidative or nitrosative stress.[120]

ARG1-mediated arginine depletion can downregulate the TCR ζ chain (CD3ζ) and raise the T-cell activation threshold.[121,122] ROS/NO can further impair TCR signaling and effector functions[120], whereas immunosuppressive cytokines such as IL-10 and TGF-β can promote Treg expansion/recruitment and attenuate DC licensing.[120,123] In a comparative study of TLS in HPV-associated cervical cancer and head and neck squamous cell carcinoma, cervical cancer TLS were skewed toward enrichment of Tregs and PMN-MDSCs. In fatal cases, TLSs lacked GC features and showed the highest densities of Tregs and PMN-MDSCs. These cases also had high ARG1 expression in PMN-MDSCs, reduced TCR ζ chain expression in tumor-infiltrating T cells, and no detectable HPV-specific T cells.[116]

In the TME, M1-like tumor-associated macrophages (TAMs) can help recruit and position effector and stem-like CD8$^+$ T cells by producing chemokines such as CXCL9/10/11 and CCL5. This supports close interactions with antigen-presenting cells and helps T cells enter tumors and become re-activated locally.[124–126] Such TAMs tend to express major histocompatibility complex class II (MHC-II), antigen processing/presentation pathways, and co-stimulatory molecules (e.g., CD40/CD80/CD86), and can secrete pro-inflammatory mediators that support a Th1–IFN-γ axis.[125] Conversely, immunosuppressive M2-like TAMs often show CD68$^+$ phenotypes with repair-like programs such as CD163$^+$, CD206$^+$, and C1QC$^+$. They

can express high PD-L1, secrete IL-10 and TGF-β, promote myeloid recruitment through the CCL2 to CCR2 axis, and strengthen a suppressive environment through lipid and tryptophan metabolism-related pathways.[127] Notably, M1-like and M2-like programs represent a continuum rather than a strict binary in vivo. TAM states can shift with spatial niche (e.g., tumor nests, stroma, perivascular regions), following spatially constrained transcriptional and functional trajectories.[128] These shifts are driven by local cues. IFN-γ, TLR, and CD40 signals can increase antigen presentation and inflammatory programs and push TAMs toward M1-like states. In contrast, IL-4 and IL-13, IL-10 and TGF-β, colony-stimulating factor (CSF)-1-axis signaling, and hypoxia or metabolic stress can increase repair and immunosuppressive programs and push TAMs toward M2-like states.[129,130]

In a multicenter cohort of gastric-type cervical adenocarcinoma (GAC) (n=153), the tumor immune microenvironment (TIME) was characterized by T-cell paucity and macrophage enrichment. Advanced/progressive cases showed more pronounced infiltration of M2-polarized macrophages. The study further reported that TLS-positive cases were accompanied by increased immunosuppressive infiltrates such as Tregs, and that mature TLS correlated with poor prognosis.[131] Similarly, in an untreated soft-tissue sarcoma cohort (n=31), spatial analyses suggested that IL17A$^+$ Th17-like cells preferentially localized to mature TLS, whereas CD163$^+$ (M2-like) macrophages were enriched in immature TLS. A composite pattern of "high GC B-cell/Th17 and low M2-like macrophages" was associated with better survival.[132] Together, these findings suggest that "TLS presence with a suppressive orientation" may reflect an M2-like, macrophage-dominated environment in the surrounding TME. However, the exact mechanisms and signaling pathways that control how M2-like TAMs interact with TA-TLSs still need to be clarified.

Stromal cells and HEVs

HEV-like vessels, often marked by PNAd/MECA-79, are main entry point for circulating lymphocytes into TLSs and help keep local antitumor responses supplied with new immune cells.[82,133] In NSCLC, Xenium single-cell in situ spatial transcriptomics identified TLS-associated high endothelial cells (HECs). These cells had high ID1 expression and increased PNAd biosynthesis and adhesion-molecule programs, forming an "ID1-high, PNAd-rich" mature HEV program. Multiplex immunofluorescence validation in an independent cohort associated this HEV program with higher ICB response rates and longer survival, suggesting that molecular maturation of HEVs itself may be a key determinant of TLS functionalization and a predictor of treatment benefit.[134] In nasopharyngeal carcinoma, interferon-responsive HEVs (IFN-HEVs) were shown to promote TLS formation through secretion of chemokines such as CXCL9 and were associated with ICB responsiveness. This indicates that HEVs are not just entry routes; they can actively drive TLS formation and immune organization.[135]

Organizer-like fibroblasts and other stromal lineages can separate the T-cell zone from the B-cell follicle and set routes where immune cells stay and move. They do this by secreting homeostatic chemokines (e.g., CCL19/CCL21 and CXCL13), which shapes TLS function early in the process. In tumors, fibroblastic reticular cell (FRC)-like or LTo-like stromal programs can provide structural and signaling support for immune activation.[23,25,136] Under some microenvironment pressures, these same programs can also link to immunosuppressive pathways.[137,138]

In a humanized mouse model of colorectal cancer, CCL19$^+$ fibroblasts promoted B-cell recruitment and lymphocyte transport toward TLS via CCL19, facilitating TLS development.[25] In NSCLC, spatial data suggested that CCL19$^+$ FRC-like stromal cells not only help organize TLSs but also form continuous three-dimensional fiber networks, sometimes called "T-cell tracks." Using three-dimensional topological tracing across consecutive 10-μm sections, the authors demonstrated that these tracks spatially bridge TLS and the tumor bed. Measurements of CCL19 gradients along the tracks, together with analyses of membrane contacts between FRCs and T cells, supported two roles: guiding cell movement and providing a local niche that supports T-cell residence and differentiation.[136] In a murine melanoma TA-TLS model, the TME reactivated embryonic lymphoid organogenesis programs (e.g., TNFR/LTβR–NF-κB), enabling a subset of cancer-associated fibroblasts (CAFs) to acquire LTo-like transcriptional and functional programs. LTo-like CAFs produced CXCL13 to recruit LT$\alpha_1\beta_2^+$ B cells. The incoming B cells then promoted CAF accumulation and PDPN$^+$ reticular stromal expansion through LT$\alpha_1\beta_2$ to LTβR signaling, which increased TLS size and organization through a positive feedback loop.[23]

However, in an ex vivo co-culture model using primary CAFs from human NSCLC, CAF-derived TGF-β signaling induced a CXCL13 program in activated T cells. At the same time, it expanded Tregs and reduced IL-2 production and availability. Blocking TGF-β reduced both CXCL13 induction and Treg expansion.[138] Notably, although mature TLS (mTLS) in NSCLC are generally associated with ICI benefit, mTLS positivity does not necessarily equate to effective antitumor immunity. Integrated spatial transcriptomics and multiplex immunofluorescence suggested that two α-smooth muscle actin (SMA)$^+$ CAF programs can occur in tumors with primary resistance even when mTLSs are present. MYH11$^+$ αSMA$^+$ CAFs were linked to more TIGIT/ICOS^{hi} CD4$^+$ FoxP3$^+$ Tregs and to stromal trapping of CD8$^+$ T cells that do not enter tumor tissue. In contrast, FAP$^+$ αSMA$^+$ CAFs were linked to stronger exhaustion features in intratumoral CD8$^+$ T cells.[137]

TREATMENT-INDUCED REMODELING

TLS in chemotherapy

Across tumor types, chemotherapy can have both positive and negative effects on tertiary lymphoid structures (TLSs). Depending on the drug class, dosing route or schedule, and baseline immune and stromal flexibility, chemotherapy may trigger new TLS formation,[139] reshape existing TLSs,[140,141] or damage TLS structure.[142] Paired human tissue collected before and after treatment provides the clearest evidence of changes over time. In hepatoblastoma linked to germline APC mutations, cisplatin-based neoadjuvant chemotherapy induced intratumoral TLSs that were not seen before treatment, suggesting that platinum regimens can promote TLS formation when the immune setting is permissive.[139] In nasopharyngeal carcinoma, gemcitabine plus cisplatin (GP) increased the number of TLS-like structures or aggregates and shifted intratumoral T cells toward a more effector-friendly state.[141] In metastatic high-grade serous ovarian cancer (HGSOC), carboplatin plus paclitaxel neoadjuvant chemotherapy promoted TLS formation and maturation and was linked to higher levels of TCF1$^+$ PD-1$^+$ CD8$^+$ T cells. This is consistent with maintaining or expanding a renewable antitumor T-cell pool when the TLS niche is preserved.[140]

Regional delivery may more easily create a TLS state that supports immunotherapy. Pressurized intraperitoneal aerosol chemotherapy (PIPAC) with oxaliplatin induced immune biomarkers that included TLS-related signals.[143] In hepatocellular carcinoma (HCC), FOLFOX hepatic artery infusion chemotherapy (HAIC) was linked to higher TLS positivity and density inside tumors than in untreated controls, and higher TLS burden correlated with better treatment response and longer progression-free survival (PFS). The authors suggested that local chemotherapy-driven inflammation and tissue remodeling promote TLS formation through CXCL12-focused recruitment supported by interactions among central memory T cell （Tcm）-like CD4$^+$ T cells, MMP2$^+$ fibroblasts, and FOLR2$^+$ CCL4$^+$ macrophages.[144] Integrative single-nucleus RNA sequencing and spatial transcriptomics of paired HCC samples before treatment and after FOLFOX HAIC also suggested higher proportions and stronger communication among CD4$^+$ T cells, CD20$^+$ B cells, and DC subsets, together with TLS formation. A PD-1$^+$ GZMK$^+$ intermediate exhausted CD8$^+$ subset (Tex-int) expanded, accumulated next to TLSs, and later spread through tumors while retaining an antitumor functional profile.[145]

Conversely, chemotherapy can weaken TLS-mediated immunity by depleting lymphocytes, damaging stromal support, or preferentially reducing highly proliferative lymphoid subsets, such as germinal center B cells and cycling T cells. In this case, TLSs may still be visible but work less well. In pancreatic ductal adenocarcinoma, neoadjuvant therapy with gemcitabine plus FOLFIRINOX was linked to suppression of a B-cell-centered immune landscape and may harm TLS formation.[146] In murine pancreatic cancer, inducing TLSs markedly improved the effect of gemcitabine, supporting the idea that building a TLS niche can turn part of the cytotoxic effect into longer-lasting immune control when chemotherapy alone is not enough.[147] TLS maturity can also change with treatment. In rectal cancer, neoadjuvant treatment disrupted the structure of mature TLSs, suggesting that germinal-center-like organization can be lost even when lymphocytes remain.[142] Moreover, in lung

squamous cell carcinoma, corticosteroids given around chemotherapy impaired germinal center development and reduced TLS maturation, making TLS status less informative for prognosis even though lymphoid aggregates persisted.[46]

Mechanistically, chemotherapy may promote TLS formation and maturation through DNA damage and cellular stress, stronger inflammatory signaling and antigen presentation, improved local cooperation between T and B cells, and vascular and stromal remodeling. Several agents, such as anthracyclines and oxaliplatin, can trigger features of immunogenic cell death (ICD), including calreticulin (CALR) exposure, ATP release, high mobility group box 1 protein (HMGB1) release, and type I interferon-related programs. These changes can recruit and activate antigen-presenting cells and create an inflammatory setting that supports ectopic lymphoid organization.[148,149]

In the nasopharyngeal carcinoma GP study, experiments suggested that chemotherapy-related DNA fragments activate STING and type I interferon signaling, increase MHC-I, and induce a TLR9-dependent innate-like B cell (ILB) program. ILBs were proposed to expand Tfh and Th1 cells through ICOSL-ICOS signaling and to boost cytotoxic T lymphocytes (CTLs) within TLS-like structures that lack typical germinal centers. ILB frequency correlated with overall and disease-free survival in a phase III GP cohort.[141] In HGSOC, multi-omics analyses suggested that neoadjuvant chemotherapy induces endoplasmic reticulum stress in metastases and promotes dense immune infiltration and TLS formation. TLS maturation was associated with higher density of ICI-sensitive TCF1$^+$ PD-1$^+$ progenitor-like CD8$^+$ T cells and a shift of PD-1$^+$ CD8$^+$ cells toward a TCF1$^+$ PD-1$^+$ state located closer to tumor cells with cytotoxic features (GZMB and IFNG).[140]

HEV-related entry programs and stromal niches are also important for maintaining TLSs under chemotherapy pressure. In a murine melanoma model, the immunogenic cell death (ICD)-inducing agent doxorubicin, compared with the non-ICD agent gemcitabine, increased PNAd$^+$ HEV features and promoted TLS formation. These changes were accompanied by greater CD8$^+$ T-cell infiltration, increased tissue-resident memory T-cell features, enhanced B-cell and dendritic-cell activation, reduced Treg abundance, and higher PD-1 expression on CD8$^+$ T cells together with higher PD-L1 expression on tumor cells. Collectively, these findings suggest that ICD-associated chemotherapy can foster a more immune-active microenvironment permissive for HEV formation, while simultaneously inducing adaptive checkpoint upregulation that may support combination with PD-1/PD-L1 blockade.[150]

TLS changes may also help predict benefit under chemotherapy. In HER2-negative breast cancer, TLS-related gene signatures can predict response to neoadjuvant chemotherapy and further stratify who benefits from adding immunotherapy. This suggests that TLS programs capture pre-existing immune capacity that chemotherapy can use rather than replace.[151] Among breast cancer patients receiving neoadjuvant chemotherapy, the presence of TLSs is associated with a lower residual nodal burden in the axilla.[152] Circulating markers may also reflect immune organization near TLSs. In metastatic colorectal cancer treated with oxaliplatin-based first-line therapy, changes in serum CXCL13 over time were associated with outcomes and closely linked to tumor immune and TLS features. This suggests that lymphoid chemokines could serve as minimally invasive indicators to monitor chemotherapy-related immune remodeling.[153] However, in a retrospective study of epithelioid malignant peritoneal mesothelioma, TLS positivity was associated with receiving preoperative systemic chemotherapy, yet no significant differences in overall survival (OS) or PFS were observed. This highlights that the link between TLS structure and function can be strongly context dependent.[154]

TLS in radiotherapy

Radiotherapy can affect TLSs not only by damaging tumor cells, but also by changing local inflammation and blood vessels.[155] Evidence from animal studies and limited presurgical samples suggests that TLSs can enter a short disruption phase after irradiation and then remodel over time, with changes in abundance, maturation state, and immune-cell composition.[155–159] These findings support a transition from acute injury to longer-term TLS remodeling after irradiation

In a KP spontaneous lung tumor model, a single 11.7 Gy whole-lung dose reduced TLS numbers early, but TLSs reappeared later and became more mature, with changes in immune cell composition.[156] In another Kras-driven spontaneous lung adenocarcinoma model, whole-lung low-dose radiotherapy (LDRT, 1 Gy) increased immune cell infiltration and raised TLS formation by day 7. Compared with LDRT alone, adding anti-PD-1 further increased TLS maturation. This suggests that dose and schedule can shape TLS remodeling and how well it pairs with immunotherapy.[160]

Short-window clinical samples often show patterns consistent with a disruption phase. In resectable pancreatic ductal adenocarcinoma (PDAC), presurgical stereotactic body radiotherapy (SBRT, 25 Gy in 5 fractions) reduced tumor cell density and increased markers linked to immunogenic cell death. It also increased collagen deposition and reduced TLS numbers, while failing to clearly reduce or reprogram dominant immunosuppressive populations. This suggests that, in this regimen and tissue context, TLSs may be impaired and that dose, fractionation, and timing may need optimization.[157] In the locally advanced rectal cancer neoadjuvant setting (neoadjuvant chemoradiotherapy [NCRT] vs neoadjuvant chemotherapy [NCT]), a treated cohort (n = 221) showed lower TLS density and maturity than an untreated cohort (n = 242). TLS density was lower after NCRT than after NCT, while mTLS+ rates were not significantly different between the two treatment types.[158] In an ESCC neoadjuvant cohort covering multiple strategies (n = 359), mature TLS counts were lowest in the NCRT arm when compared with NCT, neoadjuvant immunotherapy (NCI), NCRT, and surgery-only groups.[159] In a retrospective ESCC cohort, neoadjuvant chemoradiotherapy plus immunotherapy (NRCI, n = 49), compared with neoadjuvant chemotherapy plus immunotherapy (NCI, n = 108), achieved a higher major pathological response (MPR) and improved OS and disease-free survival (DFS). It was also linked to higher proportions of CD20$^+$Ki67$^+$ proliferating B cells, CD21$^+$ dendritic cells, and CD8$^+$Ki67$^+$ and CD4$^+$Ki67$^+$ proliferating T cells within mature TLS.[161] Overall, radiotherapy-related TLS remodeling has been described mainly in animal models and short-window surgical samples. Human evidence with clear time series, dose and fractionation comparisons, and repeat sampling remains limited.

Radio-immunotherapy combinations can be viewed as a time-ordered process. Radiotherapy changes antigen supply and local vascular and inflammatory conditions, while immunotherapy removes brakes on effector circuits. Even so, immune responses vary strongly by cancer type and treatment regimen. In immunologically cold NSCLC, SBRT combined with pembrolizumab was linked to stronger interferon responses and higher antigen processing and presentation programs in non-irradiated lesions, along with systemic immune activation such as TCR clonal expansion. Some patients also showed stronger programs linked to humoral immunity, suggesting that combined therapy can mobilize both cellular and humoral immunity at distant sites in selected settings.[162] Histologic support also comes from case-level observations. An ALK$^+$ NSCLC patient with multi-line TKI resistance received SBRT to spinal metastases followed by pneumococcal vaccination and showed regression of distant lesions. Resected or biopsied samples showed strong TIL infiltration and early TLS-like structures, but this remains anecdotal evidence.[163] In longitudinal single-cell and spatial analyses of triple-negative breast cancer, some patients had baseline lymphoid and humoral features and tended to respond. Others developed stronger cytotoxic T-cell programs and antigen presentation related myeloid programs with spatial co-localization only after radio-immunotherapy. This fits with radiotherapy enabling immune activation, proliferation, and infiltration that can amplify immunotherapy effects.[164] In a glioblastoma model, fractionated RT (10 Gy in 5 fractions) induced a more than tenfold transient increase in intratumoral T-cell content , yet anti-PD-1 benefit depended on schedule. Compared with giving anti-PD-1 during radiotherapy, giving it after radiotherapy during the window when T-cell infiltration peaked produced greater benefit. The study also showed that concurrent anti-PD-1 and radiotherapy favored an immune state with TGF-beta signaling, Treg differentiation, and local proliferation, with enrichment of a CD103$^+$ (a tissue residency associated integrin marker) Treg population. This population showed higher lipid metabolism and peroxisome proliferator-activated receptor (PPAR)-related programs and stronger suppressive capacity in vitro, leading to a more exhausted CD8$^+$ T-cell state with less proliferation and cytotoxicity. Adding a Treg-targeting intervention reduced Tregs (including CD103$^+$ Tregs),

was accompanied by TLS-like structures, increased the number and activity of $CD4^+$ and $CD8^+$ T cells, and improved the combined effect of radiotherapy and immunotherapy.[165]

Mechanistically, radiotherapy can induce type I interferon through cytosolic DNA sensing and activation of the cGAS-STING axis. This process often relies on dendritic cells recognizing DNA from irradiated tumor cells, which can drive chemokine networks and amplify adaptive immunity, creating conditions that support TLS induction.[166] However, this priming is limited by a dose-threshold negative feedback. When a single-fraction dose exceeds about 12 to 18 Gy, the DNA exonuclease TREX1 increases and clears cytosolic DNA, which weakens cGAS-STING signaling and reduces immunogenicity. This suggests that fractionation and sub-threshold dosing are more likely to sustain interferon-axis amplification.[167] Consistent with this, low-dose radiotherapy, even when not mainly aimed at direct tumor killing, can trigger tumor-cell stress and DNA-damage signals and increase interferon-related inflammatory pathways and multiple chemokines in vivo. This can recruit T and NK cells and cross-presenting DCs, improve replenishment of infiltration in cold tumors, and increase sensitivity to immunotherapy combinations.[168]

Taken together, current evidence suggests that radiotherapy can either increase or reduce TLSs, depending on dose and fractionation, treated volume, and the timing of combination therapy. Future human studies with longitudinal sampling and careful dose stratification are needed to confirm TLS remodeling over time and to guide optimization of radiotherapy and immunotherapy regimens.

TLS in immune checkpoint blockade

TLS as predictive biomarkers for ICB. Across solid tumors, tertiary lymphoid structures (TLSs) have often been linked to higher response rates and better survival with immune checkpoint blockade (ICB). This supports TLSs as tissue biomarkers that capture both lymphocyte recruitment and locally organized adaptive immunity. In melanoma, multiple cohorts have consistently connected TLSs or B cell rich inflammatory phenotypes with benefit from anti-PD-1/PD-L1 or anti-CTLA-4 therapy. At both histologic and transcriptomic levels, TLS-related gene programs and B-cell infiltration have been associated with favorable outcomes and with a more immune-active tumor microenvironment.[29] Evidence from longitudinal RNA-seq deconvolution, immunohistochemistry, single-cell transcriptomics with BCR clonal analysis. In responders, intratumoral B cells tend to cluster in TLSs and show clonal expansion. Specific B-cell states, such as a higher fraction of class-switched memory B cells, have also correlated with response.[30]

In advanced soft-tissue sarcoma, the phase II PEMBROSARC study prospectively screened and stratified patients by TLS status. It found higher clinical benefit from pembrolizumab in the TLS-positive subgroup, suggesting that TLS-based stratification can add predictive information in tumor types with low overall ICB response rates.[169] In biliary tract tumors, a comparative analysis of a small cholangiocarcinoma cohort receiving immunotherapy (n = 16) reported higher objective response and disease control rates in TLS-positive patients (ORR 71% vs 0%; DCR 100% vs 67%). Spatial and transcriptomic analyses showed higher expression of B cell related genes in TLS regions and enrichment of memory B-cell and myeloid DC features. T cells in TLSs preferentially expressed genes linked to progenitor exhaustion and showed lower cytotoxicity signatures. Tumor-infiltrating lymphocytes (TILs) in TLS-positive tumors also showed higher PD-L1 and LAG-3 expression, suggesting that TLS-related immune activation can coexist with inhibitory feedback.[170]

Importantly, the predictive value of TLSs depends on spatial context, rather than on a simple TLS-positive or TLS-negative label. In resectable esophageal squamous cell carcinoma (ESCC) treated with NCI, TLSs showed different prognostic patterns by compartment. TLS abundance within the tumor and at the invasive margin correlated with better survival, whereas peritumoral TLS abundance was associated with worse outcomes under the study definition.[161] In recurrent or metastatic head and neck squamous cell carcinoma, multimodal spatial-omics analyses across two human cohorts measured TLS-to-tumor distance. This distance, together with immune-activation patterns in nearby areas, separated responders from non-responders. These results suggest that TLSs closer to the tumor bed, with greater potential to supply and support infiltration, may better reflect ICB benefit.[171]

In a retrospective gastric cancer immunotherapy cohort (n =59) that combined H&E, multiplex immunofluorescence, spatial transcriptomics, and single-cell analyses, Xie et al. proposed the concept of "tumor-core TLS (TC-TLS)." TLS presence in the tumor core correlated with improved immune-related OS (P = 0.049). It was also associated with higher densities of specific T-cell and $CD4^+$ subsets, shorter intercellular distances, and more frequent spatial proximity interactions within TC-TLS.[172] A key caveat is that current cross-cancer evidence is not sufficient to conclude that having more core or intratumoral TLSs always means stronger local immune control or better antitumor effects. Whether these patterns reflect improved immune containment or instead reflect high antigen load with chronic inflammation likely depends on cellular composition and functional readouts, and needs careful analysis rather than a single interpretation.[70]

TLS maturity can also affect predictive performance. In a larger ESCC study stratified by neoadjuvant regimens, mature TLSs were identified as an independent prognostic factor.[159] A large cross-cancer retrospective analysis further showed that mature TLSs, rather than TLS presence alone, were associated with higher objective response rates and longer PFS and OS. This association remained independent of commonly used metrics such as PD-L1 status and $CD8^+$ T-cell density, indicating that TLS maturity provides additional predictive information for ICB benefit.[173]

TLS-associated vascular entry routes can add further predictive detail. In nasopharyngeal carcinoma, spatial transcriptomics combined with a vascular single-cell atlas identified an interferon-responsive HEV state. This enabled a pretreatment predictive score that performed well across three independent ICB cohorts. The study suggested that IFN-HEVs, together with chemokine networks (for example, a CXCL9-associated axis), help shape TLS formation and immune-cell entry, linking these features to treatment efficacy.[135] In NSCLC, another study identified an HEV-like endothelial cell state with high ID1 expression within mature TLSs. This state was associated with higher response rates and better survival and remained significant in multivariable models.[134]

However, TLS presence does not always mean treatment sensitivity. In a glioma model, agonistic CD40 therapy induced TLS-like structures, but it was accompanied by a low-function T-cell state and expansion or recruitment of suppressive $CD11b^+$ B cells. As a result, efficacy was reduced when CD40 therapy was combined with checkpoint blockade, showing that inducing TLS-like structures does not automatically increase ICB sensitivity.[174] In the phase II SABR-PDL1 trial in soft-tissue sarcoma (n=61), patients received atezolizumab, with SBRT (45 Gy/3 fractions) added in cycle 2. Translational analyses showed that non-benefiters were enriched for immunosuppressive tumor-associated macrophage transcriptional features and monocyte-recruiting chemokines. A higher monocyte-to-lymphocyte ratio in tumor and peripheral blood (MonoLR) was associated with progression, and TLSs did not show stable predictive value. These results suggest that, in some tumor types and treatment combinations, a myeloid-dominant immune environment may obscure TLS-related signals.[175]

Overall, evidence across tumor types suggests that TLS-based prediction of ICB benefit should include at least three dimensions to address cases that are TLS-positive but have different outcomes. These dimensions are: (i) spatial zoning, including intratumoral versus peritumoral distribution and distance to the tumor core; (ii) maturity, such as E-TLS, PFL-TLS, and SFL-TLS; and (iii) functional modules, including HEV programs, markers of a progenitor-exhausted T-cell niche, and suppressive stromal or myeloid features.

ICB-induced remodeling of TLS. ICB can affect TA-TLS through a series of steps: releasing inhibition, reshaping inflammatory and stromal or vascular programs, and then strengthening recruitment and organization. In several mouse tumor models, Hua et al. showed that PD-(L)1 blockade reduces suppression of effector T cells and boosts local inflammatory signals, which helps activate LT and LTβR-related organizing pathways. This promotes endothelial changes toward a $PNAd^+$ HEV-like state, called tumor HEV (TU-HEV), and increases lymphocyte entry into tumors. TU-HEVs were surrounded by niches that favored $PD\text{-}1^+$ $TCF1^+$ progenitor-like $CD8^+$ T cells, supporting their further differentiation and replenishment of $GZMB^+$ $PD\text{-}1^+$ effector cells. TU-HEV maintenance required ongoing signals from $CD8^+$ T cells and NK cells, creating a reinforcing loop in which immune entry

strengthens local signals, supports HEV maintenance and expansion, and further increases immune entry and progenitor-to-effector conversion.[176]

After neoadjuvant ICB in resected HCC specimens, mature TLSs showed HEVs and evidence that $CD8^+$ T cells entered through these HEVs. This was accompanied by stronger $PDPN^+$ stromal features and close contacts between DC-$LAMP^+$ mature DCs and T cells. In tumor regression areas, involuted TLSs were observed. They had dispersed B follicles but preserved T zones, along with more DC and T-cell interactions and higher memory-related markers. These results suggest that ICB may promote the emergence or maintenance of intratumoral TLSs and may also drive later transitions toward 'memory-like, persistent presentation' TLS states after antitumor responses.[70]

However, ICB does not always increase the ability of TLSs to supply new immune cells. In an NSCLC spatial transcriptomics study, neoadjuvant ICB was linked to lower adhesion and PNAd programs in TLS-associated high endothelial cells (HECs), higher vascular remodeling signals, and fewer lymphocytes in nearby niches. This suggests that ICB can also change the molecular maturation of HEVs and reduce the efficiency of sustained immune replenishment within TLSs.[134]

In addition to vascular effects, ICB can reshape regulatory circuits within TLSs. Eschweiler et al. described tumor-infiltrating Tfr in multiple cancer types and showed that they localize within TLSs. In syngeneic mouse tumor models, anti-PD-1 treatment increased Tfr cells, whereas depleting Tfr cells before treatment with anti-CTLA-4 improved tumor control. In a retrospective melanoma cohort, sequential anti-CTLA-4 followed by anti-PD-1 was associated with improved OS, but this finding still needs prospective validation.[177]

Collectively, these findings suggest that TLS should be viewed as a dynamic and treatment-responsive ecosystem rather than a static baseline biomarker. Longitudinal evaluation of TLS quality is therefore crucial for guiding rational combination strategies. It also helps explain why clinical associations vary across different regimens and sampling time points. (Table 2)

PRECLINICAL TLS INDUCTION

Beyond clinically used chemotherapy, radiotherapy, and immune checkpoint blockade discussed above, a growing body of preclinical work has demonstrated that TA-TLS can be actively induced using engineered immunostimulatory cues, vascular remodeling, and controlled chemokine delivery to generate more mature, functional TLS-like niches.[11,12] We summarize key intervention nodes and translational delivery and clinical routes for TA-TLS induction in Figure 2.

However, most evidence comes from mouse tumor models with intratumoral administration, controlled dosing windows, and limited longitudinal human safety data under clinically realistic schedules and comorbidity backgrounds.[178,179] To move toward clinical use, key hurdles include scalable good manufacturing practice (vectors/vesicles/materials), reproducible in vivo biodistribution, and standardized readouts that confirm TLS quality rather than simply increasing lymphoid aggregates.[179,180] Safety must be addressed explicitly, because strong innate activation (e.g., STING), organizer cytokines (e.g., LIGHT/LTβR axis), and vascular modulation may provoke excessive local inflammation, systemic cytokine spillover, off-tumor ectopic lymphoid neogenesis, or autoimmune-like toxicities if delivery is not spatially constrained and titratable.[12,13,181]

Biomaterial delivery

Chemokines and organizer signals often need to form stable gradients within tumors and persist over a sufficient time window; systemic administration rarely satisfies the triad of high local concentration, low systemic exposure, and adequate duration simultaneously. Biomaterials therefore have been leveraged to convert TLS induction from a transient stimulus into an engineerable process with spatiotemporal control, increasing the probability and reproducibility of generating mature TLS, including those with GC-like features.

A locally injectable supramolecular hydrogel can form a retention depot that releases CXCL13 plus LIGHT, providing a B-cell chemotactic coordinate and an LTβR-linked organizational cue. In the B16-OVA melanoma model, this strategy increased intratumoral TLS density and the fraction of mature TLS, and synergized with PD-1 blockade.[182] Further material designs encapsulated CCL19/CCL21/CXCL13 chemokines together with organizer signals such as $LT\alpha_1\beta_2$ in lipid-coated microparticles embedded within a biodegradable thermosensitive hydrogel, enabling sustained local release over several days and inducing TLS-like structures enriched with B and T cells at injection sites, thereby enhancing antigen-specific T-cell responses in melanoma.[183]

Other strategies use the material architecture itself to provide a permissive three-dimensional niche supporting cell aggregation and interactions. A microfluidic-fabricated gelatin methacryloyl (GelMA) microporous annealed particle (MAP) scaffold that mimics to TLS sustainably recruit multiple immune cell types at postoperative tumor sites. By combining with ICBs, the scaffold elicits a stronger anticancer immune responses.[184]

'Triggerable' material platforms, such as photothermally triggered aggregation-induced emission covalent organic frameworks (AIE-COFs) and COF-306@FM, partially shift TLS induction from sustained exogenous-factor supplementation toward reprogramming of endogenous networks by inducing cytokine hypersecretion locally within tumors.[185,186] A self-transforming chitosan hydrogel can form an in situ gel near tumors and, by adsorbing DNA and related cues, promote cGAS–STING–associated inflammatory programs. It provided a more persistent upstream driver for subsequent chemokine networking and organization.[187]

Collectively, these biomaterial systems enhance the degree of organization and maturation potential of induced TLS through: (i) exogenous maintenance of chemokine gradients and time windows; (ii) provision of infiltratable three-dimensional interaction space; and (iii) coupling to endogenous innate immune pathways to drive chemokine networks and tissue remodeling. These capabilities offer actionable spatiotemporal control for rational combinations with ICB and other therapies.

Engineered delivery platforms

Biomimetic nanovesicles. Vesicle-centered delivery strategies commonly amplify local immune reprogramming by improving tissue accessibility, biasing uptake toward APCs, and prolonging intracellular signal residence, thereby providing continuous driving forces for TLS organization and maturation. BafA1@Rexo-SC comprises exosomes derived from irradiated bone marrow–derived stem cells engineered to overexpress CD47 nanobodies and STING, loaded with the autophagy inhibitor bafilomycin A1 (BafA1). Upon intracranial delivery, BafA1@Rexo-SC activated cGAS–STING signaling, induced LTo-like cells, and promoted HEV-like microvessel formation via VEGFA release, thereby inducing TLS in a murine glioma model; concurrent CD47 blockade enhanced phagocytosis and improved effector T-cell function.[188]

A biomimetic nanovesicle platform, ADU-S@M, loads the STING agonist ADU-S100 into extracellular vesicles derived from M1-polarized macrophages. After tumor entry, ADU-S@M re-polarized TAMs toward M1 and promoted DC maturation, generating abundant 'activated APCs' intratumorally. These activated APCs were proposed to act as LTi-like sources secreting LTα and TNFα and to promote tumor vascular normalization, collectively initiating de novo TLS formation.[178] Extracellular vesicles (EVs) can also be combined with hydrogels to induce TLS .Hierarchical hydrogels composed of self-assembling ferritin protein nanocages, rec1-resilin protein, and CP05 peptide efficiently anchored extracellular vesicles (EVs) and formed artificial tertiary lymphoid structures (aTLS) in mice with GC and HEV-like features.[179]

A key premise of vesicle-based platforms is therefore not a transient peak stimulus, but rather translation of innate immune activation into sustained cell–cell interactions and structured microenvironmental changes through repeat dosing and prolonged intracellular signaling, increasing the probability of generating mature TLS with HEV and GC-like features.

Viral delivery. Viral delivery platforms can integrate sustained antigen supply, local inflammatory amplification, and organizer-signal expression within a single system, extending temporal exposure through replication, durable expression, or multi-route administration. An oncolytic herpes simplex virus 1(oHSV-1) lacking ICP34.5/ICP47 markedly increased TLS density in 4MOSC1 (head and neck squamous cell carcinoma) and MC38 (colorectal cancer) subcutaneous mouse models, generating TLS-like structures characterized by clustered $CD19^+$ B cells with ordered aggregation of

Table 2. Effects of chemotherapy, radiotherapy, and immune checkpoint blockade (ICB) on TLS quantity and quality.

Treatment type	Regimen	Tumor type	TLS quantity	Maturation	Evidence type	Reference
Chemotherapy	Cisplatin-based (neoadjuvant)	Hepatoblastoma	iTLS↑ (de novo)	post-chemo follicle-like iTLS↑	Human paired (pre/post)	[139]
Chemotherapy	Gemcitabine + cisplatin	Nasopharyngeal carcinoma	TLS-like aggregates↑	GC−/no typical GC (TLS-like)	Human (clinical cohort) + mechanistic alyses	[141]
Chemotherapy	Paclitaxel + carboplatin (neoadjuvant)	HGSOC	TLS↑	Maturation↑	Human paired (pre/post) + multi-omics	[140]
Chemotherapy	Oxaliplatin-based PIPAC	CRC-PM	TLS↑ (TLS formation induced)	NA	Human (biomarker)	[143]
Chemotherapy	FOLFOX HAIC	HCC	TLS↑	NA	Human (treated vs untreated; + paired multi-omics)	[144]
Chemotherapy	Gemcitabine + FOLFIRINOX (neoadjuvant)	PDAC	TLS↓ (may harm TLS formation)	Maturation↓ (B/GC programs suppressed)	Human (neoadjuvant; observatiol)	[146]
Chemotherapy	Neoadjuvant treatment (chemoradiotherapy context)	Rectal cancer	TLS disrupted(quantity NA)	Mature TLS disrupted	Human (neoadjuvant; histology)	[142]
Chemotherapy	Peri-chemotherapy corticosteroids	Lung squamous cell carcinoma	TLS maturation↓ (quantity NA)	Maturation↓ (GC development impaired)	Human (retrospective)	[46]
Chemotherapy	Gemcitabine ± TLS induction	Pancreatic cancer	TLS↑ (with induction)	Maturation↑ (TLS induced with CXCL13/CCL21)	mice	[147]
Chemotherapy	Doxorubicin (an ICD inducer) vs gemcitabine (non-ICD inducer) vs combination of the two drugs	Melanoma	TLS↑ (ICD regimen)	Maturation↑ (HEV-like; TLS program enhanced)	mice	[150]
ICB	PD-(L)1 blockade	Mouse tumor models (multiple)	TLS↑ (with ICB)	Maturation↑ (Tpex niche supported)	mice	[176]
ICB (neoadjuvant)	Neoadjuvant ICB (unspecified)	HCC	TLS maintained/induced (NA for net change)	Mature TLS present; involuted TLS in regression areas	Human (histology)	[70]
ICB (neoadjuvant)	Neoadjuvant ICB (unspecified)	NSCLC	TLS present; region-specific abundance reported	Mature TLS: CXCL13+ follicular core	Human (spatial transcriptomics)	[134]
Radiochemotherapy+ICB (neo)	NRCI (n=49) vs NCI (n=108)	ESCC	Region-dependent: intratumoral/IM TLS↑; peritumoral TLS↑ (opposite)	Mature TLS (GC+/M-TLS)↑; NRCI enriches proliferating B/T and CD21+ DC within mTLS	Human (retrospective)	[161]
Radiotherapy	Single-dose whole-lung RT 117 Gy	lung tumor	TLS↓ early; TLS↑ later (recovery)	NA	mice	[156]
Radiotherapy	Presurgical SBRT 25 Gy/5 fractions (5 Gy × 5); surgery median 7 days (2–14) post-SBRT	Resectable PDAC	TLS↓	NA	Human short-window presurgical	[157]
Radiotherapy (neo)	NCRT vs NCT	LARC	TLS high (baseline): RFS↑; post-therapy TLS↓	Baseline maturity↑ correlates with outcome; neoadjuvant therapy: maturity↓	Human (retrospective cohorts)	[158]
Radiotherapy (neo)	NCI vs NCT vs NCRT	ESCC	TLS↓ (mature TLS counts lowest in NCRT)	Maturation↓ (mTLS lowest in NCRT)	Human (neoadjuvant cohort)	[159]
Radiotherapy ± ICB	Whole-lung LDRT 1 Gy; + anti–PD-1	lung adenocarcinoma	TLS↑ (TLS formation by day 7)	Maturation↑ (GC+ TLS↑) with LDRT + anti–PD-1	mice	[160]
Radiotherapy+ICB	SBRT + pembrolizumab	NSCLC (cold) distant lesion effects	TLS signature↑ (on-therapy, non-irradiated lesions)	NA	Human (clinical; multi-omic)	[162]
Radiotherapy+ICB (preclinical)	Fractionated RT 10 Gy/5 fractions; anti–PD-1 timing	Glioblastoma	TLS↑ with Treg targeting	NA	mice	[165]
Radiotherapy+vaccine (case)	SBRT to spine metastases + pneumococcal vaccine	ALK+ NSCLC	TLS-like structures↑ (early)	Early TLS-like (immature; GC−)	Human (case report)	[163]

Abbreviations: TLS, tertiary lymphoid structure; iTLS, intratumoral TLS; pTLS, peritumoral TLS; GC, germinal center; HEV, high endothelial venule; PNAd, peripheral node addressin (MECA-79); ICB/ICI, immune checkpoint blockade/inhibitor; ICD, immunogenic cell death; PDAC, pancreatic ductal adenocarcinoma; NSCLC, non-small cell lung cancer; ESCC, esophageal squamous cell carcinoma; HCC, hepatocellular carcinoma; SBRT, stereotactic body radiotherapy; RT, radiotherapy; LDRT, low-dose radiotherapy; NCT, neoadjuvant chemotherapy; NCRT, neoadjuvant chemoradiotherapy; NCI, neoadjuvant chemotherapy plus immunotherapy; NRCI, neoadjuvant radiochemotherapy plus immunotherapy; Treg, regulatory T cell; Tfr/TFR, follicular regulatory T cell; TAM, tumor-associated macrophage; MDSC, myeloid-derived suppressor cell; Tfh, T follicular helper cell; Tpex, progenitor-exhausted T cell; ORR, objective response rate; OS, overall survival; PFS, progression-free survival; DFS, disease-free survival; RFS, recurrence-free survival; MPR, major pathologic response; pCR, pathologic complete response; HGSOC, high-grade serous ovarian cancer; LARC, locally advanced rectal cancer; KP, Kras;Trp53 (Kras/p53); CRC, colorectal cancer; CRC-PM, colorectal cancer peritoneal metastasis; TNBC, triple-negative breast cancer; APC, adenomatous polyposis coli; ALK, anaplastic lymphoma kinase; TKI, tyrosine kinase inhibitor; NAC/NACT, neoadjuvant chemotherapy; HAIC, hepatic arterial infusion chemotherapy; GP, gemcitabine plus cisplatin; PIPAC, pressurized intraperitoneal aerosol chemotherapy; NA, not available

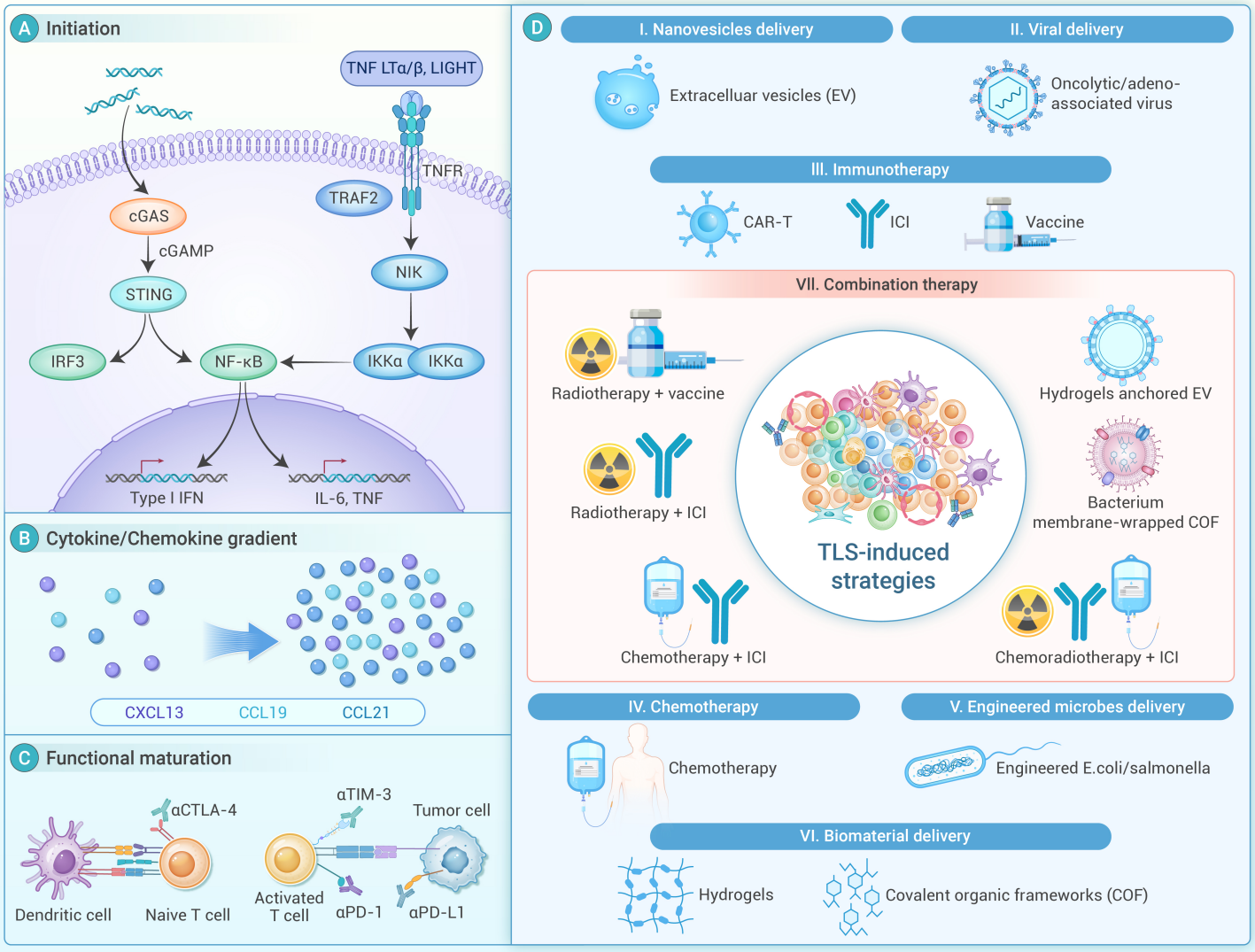

Figure 2. TA-TLS induction: key intervention nodes (A–C) and representative strategies (I–VII) This schematic summarizes representative preclinical approaches for inducing tumor-associated tertiary lymphoid structures (TA-TLSs). (A–C) indicate major intervention nodes commonly targeted during TA-TLS induction: (A) Initiation, therapy- or stress-triggered inflammatory activation that primes stromal and vascular organizer programs; (B) Cytokine/chemokine gradients, establishment of homeostatic cues, including CXCL13 and CCL19/CCL21, that recruit and spatially organize CXCR5$^+$ B cells, CCR7$^+$ T cells, and dendritic cells; and (C) Functional maturation, reinforcement of antigen presentation, T-cell priming, and effector activation, which may be further supported by immune checkpoint modulation. I–VII depict representative therapeutic platforms and treatment modalities for TA-TLS induction, including (I) nanovesicle/extracellular vesicle delivery, (II) viral delivery, (III) immunotherapy, (IV) chemotherapy-based regimens, (V) engineered microbe delivery, (VI) biomaterial delivery, and (VII) combination strategies.

CD3$^+$/CD8$^+$ T cells and enrichment of TCF1$^+$ stem-like CD8$^+$ T cells. The authors noted upregulation of TLS-related chemokines and reinforcement of the CXCL10–CXCR3 axis, and blockade of CXCL10/CXCR3 attenuated TLS formation; oHSV combined with anti-PD-1 conferred greater benefit.[189]

Endothelial-targeted adeno-associated virus (AAV)-LIGHT drove local expression of LIGHT/TNFSF14 on glioma vasculature, promoting reprogramming toward HEV/tumor-associated HEV phenotypes and upregulating lymphangiogenic programs, thereby inducing T cell–enriched TLS/TLS-like structures in immunotherapy-refractory murine glioma.[181] In C57BL/6 subcutaneous tumor models, intratumoral injection of an oncolytic adenovirus encoding murine IL-15 (Ad-IL15) upregulated LTα/LTβ/TNFSF14 and CCL19/CCL21/CXCL13 programs and promoted PNAd$^+$ HEVs and immune-cell aggregation via activation of the STING–TBK1–IRF3 pathway in DCs. The induced structures resembled early TLS units, with increased but relatively dispersed B220$^+$ B cells.[190]

Engineered microbes and cellular delivery. A synthetic-biology Salmonella typhimurium strain (SLC_VNP20009) equipped with a synchronized lysis circuit can colonize colorectal tumors and undergo programmed lysis to release LIGHT locally. Through binding to herpes virus entry mediator (HVEM) and particularly via activation of ILC3s, this approach promoted immune-cell aggregation and responses and supported maturation of TLS.[180] Meanwhile, an E@L-P/ICG 'photosensitive bacterial system' engineers Escherichia coli to carry LIGHT internally and decorates the bacterial surface with PLGA/ICG nanoparticles. After enrichment in an orthotopic colonic tumor model, laser triggering induces mild photothermal effects and bacterial self-lysis, enabling in situ release of antigen cues together with LIGHT and inducing the formation of HEVs.[191]

The similar strategy has also been applied in CAR-T cell therapies. By engineering prostate-specific membrane antigen -targeted CAR-T cells that secrete LIGHT (Pbbz-LV CAR-T), the study demonstrates activation of LTβR signaling, which promotes tumor vascular normalization, thereby facilitating the induction of TLS. These effects were validated in murine models of prostate cancer and melanoma.[192]

Cancer vaccine–enabled TLS induction

ACNVax (antigen-clustered nanovaccine) presents HER2 B-cell and CD4 epitopes at a high density with an optimized inter-cluster spacing (5–10 nm) on nanoparticle surfaces to enhance B cell–CD4 T-cell crosstalk. In a BALB/c subcutaneous HER2$^+$ breast cancer (D2F2/E2) model, combining ACNVax with anti–PD-1 and LIGHT upregulated lymphoid-aggregation factors includ-

ing CCL19/CCL21a/CXCL13 and yielded TLS-like structures in tumors.[193] An EBNA1-related nanovaccine coupling antigen with dual adjuvants (Mn^{2+} plus CpG) induced LTα/LTβ-associated organizational pathways and upregulated homing networks (CCL19/CCL21 and CXCL13), accompanied by TLS formation and enhanced antitumor effects.[194]

MLP-aTIM-3 delivers matched antigen and co-stimulatory cues to TIM-3^{high} tumor-infiltrating T cells. Antigens are presented as peptide–MHC (pMHC) on 'antigen-sensitized' dendritic cell membranes incorporated into the nanoparticle, and TIM-3/aTIM-3 interactions were proposed to reverse exhaustion and promote TLS formation and maturation. This effect was most evident in an orthotopic pancreatic cancer model and showed therapeutic extension to liver-metastasis and colorectal cancer models.[195]

In anatomically immune-privileged contexts, vaccine-enabled TLS induction further supports feasibility of antigen-specific priming coupled to establishment of structured local immune sites. A therapeutic protein vaccine using human cytomegalovirus (HCMV) IE1 or a detoxified mutant (IE1mut) induced local inflammation in an orthotopic GL261-IE1 glioma model, upregulated TLS-associated genes (LTα/LTβ, Cxcl13, Ccl19, and Ccl21), increased intratumoral DC and macrophage infiltration, and promoted TLS formation at the tumor margin, suggesting that even within the central nervous system, antigen-specific initiation can drive emergence of structured adaptive immune niches when local inflammation and homing cues are satisfied.[196] Three-dimensional printed porous scaffold offer a scalable spatial framework to carry immunomodulatory factors and induce artificial TLS-like structures.[197]

Vaccine-enabled TLS induction does not simply increase one cell population or one factor in a linear way. Instead, it works by meeting three local conditions at the same time: sustained antigen accessibility, innate immune–driven chemokine networking, and maturation cues. This helps turn scattered immune infiltration into structured immune niches with B/T cell compartmentalization and antigen-presentation capacity. Accordingly, testable causal chains often follow two levels: first, antigen supply together with pattern-recognition receptor (PRR) signaling pushes local inflammation and homing signals beyond a threshold; second, modulation of B-cell priming efficiency and improvement of the quality of B–T cooperation facilitate organizational maturation.

ADVANCES IN TLS DETECTION AND ANALYSIS

Digital pathology

Digital pathology turns conventional glass slides into computable high-resolution whole-slide images through whole-slide imaging (WSI), which supports computational pathology workflows.[198,199] With WSI as input, artificial intelligence (AI), especially deep learning, can automatically locate and count TLSs, assess maturation-related morphology, and build models that link TLS features to prognosis and treatment benefit.[200–204]

Several approaches have emerged. First, routine H&E-based TLS assessment is increasingly being standardized through computational methods. Training signals and datasets have expanded from single-center manual labels to multi-center retrospective cohorts and public repositories. This supports automated TLS segmentation with external validation.[200,201] For example, Chen et al. established a multicenter gene-based digital TLS score (gsTLS) for gastric cancer, using H&E-defined TLS status as the reference.[201] Second, models have moved from single-scale convolutional neural networks (CNNs) to multi-resolution designs and weakly supervised multiple-instance learning (MIL) or prototype-learning methods. These approaches aim for better transfer across cohorts and cancer types, handle sparse TLSs, and reduce the need for dense pixel-level labels.[200,205] HookNet-TLS used multi-resolution networks to measure TLS density and detect germinal centers, reaching near-expert TLS quantification across multiple cancers,[200] whereas weakly supervised MIL has been used to learn TLS-related patterns from slide-level labels when per-TLS pixel labeling is not practical.[205] Third, tasks have expanded from binary detection to maturation grading and spatial feature measurement, and these outputs have been linked to recurrence risk, immunotherapy outcomes, and adjuvant-treatment benefit.[202–204] TLS-PAT, for example, used dual-IHC (CD21/CD23) WSI in colorectal cancer to grade TLS maturation based on FDC and germinal center markers, producing outputs more consistent with biological grouping.[203] In endometrial cancer, spatial subtypes were separated using features such as distance to the tumor boundary, enabling quantitative assessment of TLS location and its association with survival and immunotherapy benefit.[204]

Despite rapid progress and many methods, key challenges remain in reproducibility, generalizability, and clinical validation. First, TLS definitions, maturation criteria, and reference labels differ across studies. H&E morphology, dual-IHC, mIHC, and spatial-omics supervision do not always mark the same structures, which makes results hard to compare and highlights the need for shared cross-center annotation standards and evaluation systems.[203] Second, differences in staining batches, scanners, and slide preparation can still change image features. Multi-resolution and weakly supervised methods can improve robustness, but cross-site use still needs clear quality control, color normalization, and external validation.[200] Third, most clinical evidence is retrospective and tool-focused. Transferable thresholds, workflow integration, prospective multi-center validation, and evaluation tethered to real clinical decision pathways are still relatively limited, constraining translation of TLS-AI metrics into broadly deployable clinical tools.[202,204]

Genomic and transcriptomic detection

When high-quality whole-slide material is unavailable, or when large multi-center cohorts require scalable screening, TLSs can be inferred from bulk RNA-seq, single-cell transcriptomics, and spatial transcriptomics by using TLS-related transcriptional programs.[3] TLS formation is linked to local activation of lymphoid organ development programs, including higher expression of lymphocyte homing and compartmentalization pathways (for example, CCR7 with CCL19/CCL21 and CXCR5 with CXCL13), lymphotoxin signaling (LTα/β), and genes related to antigen presentation and GC reactions. Together, these signals can be used to approximate structured immune niches even when tissue morphology is not available.[3]

At the bulk transcriptomic level, one of the earliest and most widely used methods is the "12-chemokine (12-CK)" signature, which uses 12 chemokine genes (CCL2, CCL3, CCL4, CCL5, CCL8, CCL18, CCL19, CCL21, CXCL9, CXCL10, CXCL11, and CXCL13) to capture TLS-like inflammation and lymphocyte homing programs across pan-cancer cohorts.[206,207] The 12-CK approach was later turned into a cross-platform transcriptional score and, in multiple cohorts, was associated with higher immune infiltration, better survival outcomes, and ICB benefit in selected tumor types. It is therefore often used as a first-pass way to screen for TLS-enriched samples in large retrospective datasets.[208]

Beyond 12-CK, single-cell and spatial multi-omics have enabled transcriptomic signatures aimed at specific TLS maturation stages and functional states. For example, in oral squamous cell carcinoma, a three-gene set (IL7, LTB, and CXCL13) based on lymphoid-neogenesis factors has been used to indicate activation of lymphoid organ development programs and was associated with TLS grading and prognosis.[209] In ovarian cancer meta-cohorts, a nine-gene TLS signature has been proposed and linked to a more inflamed immune microenvironment, reduced immune evasion, and possible immunotherapy benefit.[210]

Spatial transcriptomics has also supported signatures that treat TLSs as spatial tissue units. In triple-negative breast cancer (TNBC), a spatially derived TLS-ST 30-gene panel was built to track follicle and T-zone organization and maturation programs on tissue sections, and the panel was then applied to bulk cohorts for quantification.[6,211] In HGSOC, GeoMx digital spatial profiling (DSP) comparisons of TLS ROIs and non-TLS ROIs produced a 20-gene "TLS-DSP" signature that highlights molecular features linked to lymphocyte recruitment, activation, and tissue residence within TLS regions.[212] More cross-cancer signatures are also emerging. SpaTopic derived a TLS-25 core gene set from primary liver cancer spatial data to serve as a general TLS module for distinguishing degrees of immune organization across spatial regions.[6,213] RMYY-TLS (CXCL13, CCL19, MS4A1, LTB, CD37, CORO1A, IKZF1) combines single-cell results, spatial information, and survival links to provide a compact and reproducible TLS classification tool across cohorts.[214]

For the clinically important question of GC presence and maturation, a 29-gene "TLS imprint" signature, built around plasma-cell differentiation and immunoglobulin-gene enrichment, has been used in renal cell carcinoma and

other tumors to quantify the B-cell maturation to plasma-cell axis within TLSs.[107] Later work comparing gene sets for identifying mature TLSs (mTLSs) suggested that imprint-based signatures may perform better than broader TLS gene sets for distinguishing mTLSs. This provides a transcriptomic way to move from "TLS presence" to "TLS functional subtyping."[83] In practice, simpler surrogates such as CXCL13 alone have been used to track TLS burden and predict immunotherapy response in public muscle-invasive bladder cancer (MIBC) cohorts, although specificity and maturity resolution remain limited.[215] In clinical prediction models, TLS-related transcriptional signatures have added stratification value in immunotherapy trials. For example, a TLS signature was proposed to add predictive information among PD-L1-negative patients in the ORIENT-11 randomized trial for advanced NSCLC, with potential value independent of PD-L1. This suggests that transcriptomic TLS metrics could serve as scalable companion diagnostic candidates alongside pathology-based assessment.[216]

It should be emphasized that gene signatures are proxy measures that reflect TLS-associated cell composition and activation. They generally cannot reliably separate diffuse lymphocyte infiltration from mature TLSs with clear B and T compartments, FDC networks, and GC reactions. For translational use, cross-validation with pathology or spatial-omics readouts is usually needed.[3]

Radiomics-based TLS prediction

From a mechanistic view, TLSs are organized immune niches. Their formation often comes with local changes in blood vessels, stromal structure, and immune-cell density.[40] These microenvironment changes can show up on imaging as differences in contrast enhancement, higher texture heterogeneity inside the tumor, and changes around the tumor (for example, rim enhancement, rougher texture, and shifts in gray-level patterns).[217] Imaging can cover the whole tumor and nearby tissue, can be repeated, and is useful for preoperative evaluation and for monitoring during treatment.[218,219] Recent radiomics-based models suggest that intratumoral TLS status may be estimated non-invasively across multiple solid tumors (Table 3)

CT and PET/CT. For noninvasive TLS assessment, CT radiomics usually uses contrast-enhanced CT, and some studies also define a ring-shaped peritumoral region of interest (ROI) to capture microenvironment signals220. After segmentation and basic preprocessing (for example, resampling and intensity normalization), features such as first-order histograms, shape measures, and texture features (GLCM, GLRLM, GLSZM, GLDM, etc.) are extracted from region of interests (ROIs) or volume of interests (VOIs). Feature selection methods are then applied before model building (for example, logistic regression, support vector machine, random forest, or ensemble methods) to predict TLS presence, spatial patterns, or recurrence-related outcomes.[220–222]

In intrahepatic cholangiocarcinoma (ICC), Xu et al. combined portal-venous-phase CT radiomic features with clinical variables to build a nomogram that predicts TLS status and recurrence-free survival (RFS) (AUC = 0.88). It performed better than the radiomics-only model (AUC = 0.86) and the clinical-only model (AUC = 0.71).[221] In hepatocellular carcinoma (HCC), Wu et al. combined arterial-phase and portal-venous-phase contrast-enhanced CT radiomics with clinical variables to build a machine-learning model for noninvasive assessment of intratumoral TLS (AUC = 0.947 in training; 0.909 in validation).[223] In thoracic settings, where breathing motion, lung background, and protocol differences are more common, CT radiomics can still provide reusable preoperative models to distinguish TLS status.[220,222] In stage I lung adenocarcinoma (LUAD), Zhao et al. developed a multimodal Radiomics Integrated TLS System (RAITS). It used a three-dimensional U-shaped convolutional neural network (3D U-Net) for automatic tumor segmentation and tested radiomic and deep-learning features across peritumoral expansions of 2, 4, 6, and 8 mm. The model achieved an external AUC of 0.78 and suggested that peritumoral ROIs may better capture TLS-related microenvironment differences.[220]

Metabolic imaging provides another way to capture functional immune activation beyond contrast-enhanced CT. The signal in 18F-FDG PET/CT reflects increased glucose use in both tumor cells and activated immune cells, and activated immune cells can also show higher FDG uptake.[224,225] In pancreatic ductal adenocarcinoma (PDAC), Yan et al. analyzed 266 patients who had 18F-FDG PET/CT followed by surgical resection and found a significant positive correlation between SUVmax and TLS presence. GLUT3 and GLUT10 were higher in high-TLS-score groups and correlated with TLS scores based on the 12-chemokine signature. These results suggest that imaging features related to glucose transport and metabolism may act as indirect indicators of TLS-associated immune states. However, this approach mainly reflects functional immune activation, and its prognostic meaning across different TLS definitions and treatment settings needs larger cohorts and standardized labels.[226]

MRI. Compared with CT, MRI offers better soft-tissue contrast and functional sequences, which can help capture peritumoral immune structures in solid organs such as the hepatobiliary system. MRI-based radiomics or machine-learning models use multi-parametric sequences to measure tissue heterogeneity and vascular and stromal remodeling, using pathology (H&E whole slides or histologic review) as the reference standard for TLS detection.[227–230] Existing studies include models for intratumoral TLS (iTLS),[227–229] models that stratify peritumoral TLS (pTLS) density,[56] and approaches that combine the intratumoral core with peritumoral ring information to improve performance.[230,231]

For tumor segmentation, the most common approach is still manual contouring guided by radiologists.[6,19] Some workflows create peritumoral rings by automatically expanding the manually drawn tumor core to form layered peritumoral bands. This is a semi-automated ROI method rather than fully automated segmentation.[29] In addition to standard T1 and T2, DWI, and dynamic contrast enhancement, MRI sequences such as susceptibility-weighted imaging (SWI)[232] and intravoxel incoherent motion diffusion-weighted imaging (IVIM-DWI)[233] have been added to models predicting HCC iTLS. SWI is sensitive to small vessels and microbleeds and may provide indirect signals of microvascular changes and inflammatory activity linked to TLS,[232] whereas DWI and IVIM provide diffusion and microperfusion information that complements structural TLS readouts and can improve model interpretation.[233]

For model building, some studies add clinical and imaging variables, as well as transfer-learning features, to improve prediction performance.[227,228,234,235] In gallbladder cancer, Xu et al. used logistic regression to identify independent clinical and imaging predictors (tumor height, liver invasion, and arterial-phase hypoenhancement) and combined them with a Rad-score in a radiomics and clinical fusion model for preoperative TLS prediction (AUC = 0.891), which performed better than the clinical model (AUC = 0.870) and the radiomics model (AUC = 0.775).[228] In HCC, PyRadiomics features and transfer-learning features (e.g., ResNet50 pretrained on ImageNet) were combined to build transfer-learning radiomic (TLR) models for iTLS diagnosis, and these models showed stable performance in four-center external validation.[227] To address concerns about limited interpretability in nonlinear ensemble models (e.g., random forest and XGBoost), SHAP (Shapley Additive Explanations) can estimate each feature's contribution for an individual case and rank contributions at the cohort level.[230,232] For example, in an HCC SWI radiomics study, SHAP highlighted top contributors to iTLS positivity (e.g., logarithm_firstorder_Minimum and exponential_glszm_Zone Entropy),[232] and in a TNBC rTLS model, SHAP-based ranking supported correlation analyses between key radiomic features and pathological heterogeneity across high and low rTLS groups.[230]

Current limitations mainly involve reproducibility and use across sites. For CT, differences in scanning protocols across sites (slice thickness, tube voltage and current, reconstruction kernels, and contrast injection and timing) can strongly affect the stability of texture features and create domain shift.[236,237] For MRI, differences in field strength, sequence settings, and enhancement timing can lead to inconsistent intensity scales and feature drift, which weakens cross-cohort generalization. External validation should therefore use truly diverse devices and protocols, and should consider feature standardization and harmonization.[238,239] Segmentation errors and limited agreement between readers can also change key features, so robustness checks using repeated segmentation and stability filtering are often needed.[227,228] Peritumoral ROI thickness, expansion methods, and whether to exclude vessels, bronchi, pleura, or necrotic regions are not standardized, which reduces comparability and model portability.[228,230] Finally, most studies are retrospective and do not incorporate TLS maturation, and pathological

Table 3. Radiomics-based models for predicting intratumoral tertiary lymphoid structures (TLS) in solid tumors.

Imaging modality	Cancer type	Sample size (n)	Model formulation	Sequences / phases	Clinical purpose	Performance	Reference
CT	ICC	166	Radiomics nomogram: contrast-enhanced CT radiomics model + clinical model	Arterial (CE-CT)	Predict intratumoral TLS status and stratify postoperative RFS risk	AUC(Tr/Ext): 0.85/0.88	[221]
	HCC	171	Three-model comparison: clinical model, arterial+portal venous phase CE-CT radiomics model, and a fused machine-learning model (nomogram)	Arterial + portal venous (CE-CT)	Predict intratumoral TLS expression (TLS+ vs TLS-)	AUC (Tr/Int): 0.947/0.909	[223]
	IA	456	Chest CT radiomics model: VB-Net automatic segmentation + SVM classifier	Chest CT	Predict TLS status in invasive lung adenocarcinoma (TLS-high vs TLS-low)	AUC(Val/Int/Ext): 0.781/0.804/0.747	[220]
PET/CT	PAAD	266	18F-FDG PET/CT metabolic assessment: SUVmax associated with intratumoral TLS presence	18F-FDG PET/CT	Assess intratumoral TLS on 18F-FDG PET/CT; correlate FDG uptake with immune infiltration	SUVmax higher in TLS+; no OS association	[226]
MRI	HCC	332	Radiomics nomogram:Gd-EOB-DTPA–enhanced multiparametric MRI radiomics signature + clinical–imaging factors	T1WI, T2WI, AP, PVP, ADC, HBP	Predict intratumoral TLS positivity; stratify postoperative DFS and evaluate benefit from targeted/immunotherapy	AUC(Tr/Int/Ext): 0.860/0.823/0.875	[234]
		477	Explainable SWI radiomics model: compared LR/RF/SVM/XGBoost/KNN with SHAP interpretation	SWI	Predict HCC intratumoral TLS (iTLS+ vs iTLS-) and support identification of patients potentially benefiting from TKI-ICI	AUC (Val): 0.771	[232]
		168	IVIM multimodal nomogram: radiomics features + clinical–imaging variables+ IVIM parameters	IVIM	Predict HCC intratumoral TLS and assess RFS	AUC (Test): 0.86	[233]
		660	Multiregional MRI radiomics classifier: fusion of intratumoral and peritumoral ROI features	T2WI	Predict high pTLS density in HCC and stratify OS/RFS and immunotherapy response	AUC (Ext): 0.91	[56]
		660	Transfer-learning radiomics (TLR) model: integrated deep-learning feature score with handcrafted radiomics score	T2WI, AP, PVP	Predict intratumoral TLS in HCC; evaluate OS/RFS and response to anti–PD-(L)1 plus anti-angiogenic combination therapy	AUC(Tr/Int/Ext): 0.91/0.85/0.85	[227]
	STS	302	MRI radiomics models:	NR	Predict intratumoral TLS in STS and stratify PFS	AUC(Tr/Int/Ext): 0.878/0.778/0.772	[228]
	ICC	192	MRI radiomics signature: manual VOIs on T2WI/DWI/PVP;	T2WI, DWI, PVP	Preoperatively predict intratumoral TLS status in ICC; stratify RFS risk	AUC(Tr/Int/Ext):0.85/0.81/0.84	[235]
	GBC	173	Multiparametric MRI combined model: radiomics Rad-score integrated with clinical–imaging variables	T1WI, T2WI, DWI, AP, PVP, DP	Predict intratumoral TLS in gallbladder cancer and stratify postoperative RFS and immunotherapy OS	AUC(Tr/Ext): 0.891/0.885	[231]

Abbreviations: CT, computed tomography; CE-CT, contrast-enhanced computed tomography; MRI, magnetic resonance imaging; PET/CT, positron emission tomography/computed tomography; PAAD, pancreatic adenocarcinoma; ICC, intrahepatic cholangiocarcinoma; HCC, hepatocellular carcinoma; IA, invasive adenocarcinoma (lung); STS, soft tissue sarcoma; GBC, gallbladder cancer; TLS, tertiary lymphoid structures; iTLS, intratumoral TLS; pTLS, peritumoral TLS; AUC, area under the receiver operating characteristic curve; OS, overall survival; RFS, recurrence-free survival; DFS, disease-free survival; PFS, progression-free survival; VOI, volume of interest; ROI, region of interest; NR, not reported; AP, arterial phase; PVP, portal venous phase; DP, delayed phase; T1WI/T2WI, T1-/T2-weighted imaging; DWI, diffusion-weighted imaging; ADC, apparent diffusion coefficient; HBP, hepatobiliary phase; SWI, susceptibility-weighted imaging; IVIM, intravoxel incoherent motion; 18F-FDG, fluorine-18 fluorodeoxyglucose; SUVmax, maximum standardized uptake value; VB-Net, V-Net-based segmentation network; SVM, support vector machine; LR, logistic regression; RF, random forest; XGBoost, extreme gradient boosting; KNN, k-nearest neighbors; SHAP, Shapley additive explanations; mRMR, minimum redundancy maximum relevance; LASSO, least absolute shrinkage and selection operator; GLCM/GLRLM/GLSZM/GLDM/NGTDM, texture matrices; AJCC, American Joint Committee on Cancer; ALBI, albumin-bilirubin; Gd-EOB-DTPA, gadoxetate disodium; TKI, tyrosine kinase inhibitor; ICI, immune checkpoint inhibitor; PD-(L)1, programmed cell death protein 1 / programmed death-ligand 1

labeling may also be affected by sampling bias and spatial mismatch.[40,227] Because imaging ROIs do not perfectly match true TLS locations, higher-quality prospective multi-center cohorts, standardized ROI protocols, and spatially registered labels, potentially complemented by functional imaging such as PET/CT, are important for building interpretable and generalizable clinical tools.[226,228]

CONCLUSION

In summary, TA-TLS are not merely lymphocyte aggregates. TA-TLS should be interpreted as organized, dynamic immune niches rather than generic lymphocyte aggregates. Their clinical and mechanistic value depends on whether they establish sustained cellular influx (via HEV-like vessels), supportive stromal scaffolds, and homeostatic chemokine networks, and whether they complete key organizational elements such as T/B compartmentalization, follicular dendritic cell (FDC) networks, and GC-like reactions. The HEV–stroma–chemokine axis and the GC program constitute core structural determinants of durable immune output.[6] TLS can serve as niches for regenerative expansion and differentiation of T cells; however, when terminally exhausted lineages or suppressive modules dominate locally, the incremental benefit to immune checkpoint blockade (ICB) may be constrained.[3] Spatial localization shapes antigen load, the vascular–stromal framework, and the inflammatory background. Therefore, intratumoral and peritumoral TLS should not be merged in interpretation without explicit spatial annotation.[6] B-cell maturation and humoral outputs are integral components of TLS function, and in situ B-cell maturation and plasma-cell generation within TLS have been associated with ICB responses.[8,30] Accordingly, translational endpoints for TLS induction should prioritize restoration of structured function—encompassing 'input–priming–output'—rather than merely increasing inflammatory recruitment or immune-cell accumulation.[6]

Therapy can also remodel TLS over time. Chemotherapy and radiotherapy may induce, reshape, or disrupt TLS depending on regimen, dose and fractionation, treated volume, and sequencing. ICB can further remodel TLS through vascular and stromal programs and by reshaping regulatory circuits within TLS niches. These dynamics help explain divergent clinical associations across cohorts and highlight the need for time-resolved evaluation rather than single time-point labeling.[240]

The collective evidence supports that tumor subsets enriched for mature TLS is more likely to exhibit stronger antitumor immune cooperation and greater benefit from ICB. Nonetheless, this association is substantially modulated by tumor type, spatial niche, and inhibitory feedback modules.[29] Therefore, when TLS are used for prognostic or predictive stratification, reliance on binary TLS-positive/TLS-negative labels or a single gene signature should be avoided. Instead, quantitative readouts incorporating maturation, spatial position, and effector versus suppressive composition should be integrated to improve cross-cohort reproducibility.[6]

Looking forward, TLS research should advance on three levels. First, cross-center reusable minimal pathology marker panels and staging criteria should be established and linked to jointly calibratable readouts with digital pathology and spatial-omics platforms. Second, through longitudinal paired sampling, therapy-induction experiments, and causal-intervention models, 'bystander-associated TLS' should be distinguished from 'driver TLS,' and causal chains connecting TLS maturation trajectories with immunotherapy benefit should be defined. Third, in clinical settings, the most immediate opportunities lie in integrating TLS assessment into biomarker workflows for patient stratification, especially in immunotherapy settings, and in developing mechanism-guided combinations that actively promote high-quality TLS formation. However, several challenges remain before widespread translation is feasible, including the lack of standardized pathology criteria, inter-platform variability across digital pathology and spatial omics, uncertainty regarding the safety of TLS-inducing approaches, and the need for prospective longitudinal validation. Addressing these issues will be essential for converting TLS from an informative research feature into a robust clinical tool and therapeutic target.

REFERENCES

1. Wang Q. and Wu X. (2017). Primary and acquired resistance to PD-1/PD-L1 blockade in cancer treatment. *Int. Immunopharmacol.* **46**:210–219. DOI:10.1016/j.intimp.2017.03.015
2. Chen D.S. and Mellman I. (2013). Oncology meets immunology: The cancer-immunity cycle. *Immunity* **39**:1–10. DOI:10.1016/j.immuni.2013.07.012
3. Schumacher T.N. and Thommen D.S. (2022). Tertiary lymphoid structures in cancer. *Science* **375**:eabf9419. DOI:10.1126/science.abf9419
4. Dieu-Nosjean M.-C., Goc J., Giraldo N.A., et al. (2014). Tertiary lymphoid structures in cancer and beyond. *Trends Immunol.* **35**:571–580. DOI:10.1016/j.it.2014.09.006
5. Teillaud J.-L., Houel A., Panouillot M., et al. (2024). Tertiary lymphoid structures in anticancer immunity. *Nat. Rev. Cancer* **24**:629–646. DOI:10.1038/s41568-024-00728-0
6. Deng S., Chen Y., Song B., et al. (2025). Tertiary lymphoid structures in cancer: Spatiotemporal heterogeneity immune orchestration, and translational opportunities. *J. Hematol. Oncol.* **18**:97. DOI:10.1186/s13045-025-01754-7
7. Petitprez F., De Reyniès A., Keung E.Z., et al. (2020). 318 B cells are associated with survival and immunotherapy response in sarcoma. *Nature* **577**:556–560. DOI:10.1038/s41586-019-1906-8
8. Fridman W.H., Meylan M., Pupier G., et al. (2023). Tertiary lymphoid structures and B cells: An intratumoral immunity cycle. *Immunity* **56**:2254–2269. DOI:10.1016/j.immuni.2023.08.009
9. Randall T.D., Carragher D.M. and Rangel-Moreno J. (2008). Development of secondary lymphoid organs. *Annu. Rev. Immunol.* **26**:627–650. DOI:10.1146/annurev.immunol.26.021607.090257
10. Zhao L., Jin S., Wang S., et al. (2024). Tertiary lymphoid structures in diseases: Immune mechanisms and therapeutic advances. *Signal Transduct. Target. Ther.* **9**:225. DOI:10.1038/s41392-024-01947-5
11. Johansson-Percival A. and Ganss R. (2021). Therapeutic induction of tertiary lymphoid structures in cancer through stromal remodeling. *Front. Immunol.* **12**:674375. DOI:10.3389/fimmu.2021.674375
12. Chelvanambi M., Fecek R.J., Taylor J.L., et al. (2021). STING agonist-based treatment promotes vascular normalization and tertiary lymphoid structure formation in the therapeutic melanoma microenvironment. *J. Immunother. Cancer* **9**:e001906. DOI:10.1136/jitc-2020-001906
13. Sawada J., Kikuchi Y., Duah M., et al. (2025). Simultaneous STING and lymphotoxin-β receptor activation induces B cell responses in tertiary lymphoid structures to potentiate antitumor immunity. *Nat. Immunol.* **26**:1766–1780. DOI:10.1038/s41590-025-02259-8
14. Jeucken K.C.M., Koning J.J., Mebius R.E., et al. (2019). The role of endothelial cells and TNF-receptor superfamily members in lymphoid organogenesis and function during health and inflammation. *Front. Immunol.* **10**:2700. DOI:10.3389/fimmu.2019.02700
15. Yu H., Lin L., Zhang Z., et al. (2020). Targeting NF-κB pathway for the therapy of diseases: Mechanism and clinical study. *Signal Transduct. Target. Ther.* **5**:209. DOI:10.1038/s41392-020-00312-6
16. Bénézech C., Mader E., Desanti G., et al. (2012). Lymphotoxin-β receptor signaling through NF-κB2-RelB pathway reprograms adipocyte precursors as lymph node stromal cells. *Immunity* **37**:721–734. DOI:10.1016/j.immuni.2012.06.010
17. Sun S.-C. (2017). The non-canonical NF-κB pathway in immunity and inflammation. *Nat. Rev. Immunol.* **17**:545–558. DOI:10.1038/nri.2017.52
18. Lin L., Hu X., Zhang H., et al. (2019). Tertiary lymphoid organs in cancer immunology: Mechanisms and the new strategy for immunotherapy. *Front. Immunol.* **10**:1398. DOI:10.3389/fimmu.2019.01398
19. Amisaki M., Zebboudj A., Yano H., et al. (2025). IL-33-activated ILC2s induce tertiary lymphoid structures in pancreatic cancer. *Nature* **638**:1076–1084. DOI:10.1038/s41586-024-08426-5
20. Grogan J.L. and Ouyang W. (2012). A role for Th17 cells in the regulation of tertiary lymphoid follicles. *Eur. J. Immunol.* **42**:2255–2262. DOI:10.1002/eji.201242656
21. Chaurio R.A., Anadon C.M., Lee Costich T., et al. (2022). TGF-β-mediated silencing of genomic organizer SATB1 promotes tfh cell differentiation and formation of intratumoral tertiary lymphoid structures. *Immunity* **55**:115–128.e9. DOI:10.1016/j.immuni.2021.12.007
22. Liu W., You W., Lan Z., et al. (2024). An immune cell map of human lung adenocarcinoma development reveals an anti-tumoral role of the tfh-dependent tertiary lymphoid structure. *Cell Rep. Med.* **5**:101448. DOI:10.1016/j.xcrm.2024.101448
23. Rodriguez A.B., Peske J.D., Woods A.N., et al. (2021). Immune mechanisms orchestrate tertiary lymphoid structures in tumors via cancer-associated fibroblasts. *Cell Rep.* **36**:109422. DOI:10.1016/j.celrep.2021.109422
24. Shen S., Cui Y., Li M., et al. (2025). Toll-like receptor agonists promote the formation of tertiary lymphoid structure and improve anti-glioma immunity. *Neuro-Oncol.* **27**:140–154. DOI:10.1093/neuonc/noae167
25. Zhang Y., Liu G., Zeng Q., et al. (2024). CCL19-producing fibroblasts promote tertiary lymphoid structure formation enhancing anti-tumor IgG response in colorectal cancer liver metastasis. *Cancer Cell* **42**:1370–1385.e9. DOI:10.1016/j.ccell.2024.07.006
26. Ware M.B., Wolfarth A.A., Goon J.B., et al. (2022). The role of interleukin-7 in the formation of tertiary lymphoid structures and their prognostic value in gastrointestinal cancers. *J. Immunother. Precis. Oncol.* **5**:105–117. DOI:10.36401/JIPO-22-10
27. Rangel-Moreno J., Carragher D.M., De La Luz Garcia-Hernandez M., et al. (2011).

The development of inducible bronchus-associated lymphoid tissue depends on IL-17. *Nat. Immunol.* **12**:639–646. DOI:10.1038/ni.2053
28. Gu X., Li D., Wu P., et al. (2024). Revisiting the CXCL13/CXCR5 axis in the tumor microenvironment in the era of single-cell omics: Implications for immunotherapy. *Cancer Lett.* **605**:217278. DOI:10.1016/j.canlet.2024.217278
29. Cabrita R., Lauss M., Sanna A., et al. (2020). Tertiary lymphoid structures improve immunotherapy and survival in melanoma. *Nature* **577**:561–565. DOI:10.1038/s41586-019-1914-8
30. Helmink B.A., Reddy S.M., Gao J., et al. (2020). B cells and tertiary lymphoid structures promote immunotherapy response. *Nature* **577**:549–555. DOI:10.1038/s41586-019-1922-8
31. Ahmed A., Springfeld C. and Halama N. (2025). De novo induction of tertiary lymphoid structures: An immunotherapeutic strategy in pancreatic cancer. *Signal Transduct. Target. Ther.* **10**:173. DOI:10.1038/s41392-025-02260-5
32. Vella G., Guelfi S. and Bergers G. (2021). High endothelial venules: A vascular perspective on tertiary lymphoid structures in cancer. *Front. Immunol.* **12**:736670. DOI:10.3389/fimmu.2021.736670
33. Vella G., Hua Y. and Bergers G. (2023). High endothelial venules in cancer: Regulation, function, and therapeutic implication. *Cancer Cell* **41**:527–545. DOI:10.1016/j.ccell.2023.02.002
34. Johansson-Percival A., He B., Li Z.-J., et al. (2017). De novo induction of intratumoral lymphoid structures and vessel normalization enhances immunotherapy in resistant tumors. *Nat. Immunol.* **18**:1207–1217. DOI:10.1038/ni.3836
35. Fleig S., Kapanadze T., Bernier-Latmani J., et al. (2022). Loss of vascular endothelial notch signaling promotes spontaneous formation of tertiary lymphoid structures. *Nat. Commun.* **13**:2022. DOI:10.1038/s41467-022-29701-x
36. Heesters B.A., Chatterjee P., Kim Y.-A., et al. (2013). Endocytosis and recycling of immune complexes by follicular dendritic cells enhances B cell antigen binding and activation. *Immunity* **38**:1164–1175. DOI:10.1016/j.immuni.2013.02.023
37. Anania J.C., Westin A., Adler J., et al. (2021). A novel image analysis approach reveals a role for complement receptors 1 and 2 in follicular dendritic cell organization in germinal centers. *Front. Immunol.* **12**:655753. DOI:10.3389/fimmu.2021.655753
38. Chen Y., Wu Y., Yan G., et al. (2024). Tertiary lymphoid structures in cancer: Maturation and induction. *Front. Immunol.* **15**:1369626. DOI:10.3389/fimmu.2024.1369626
39. Cui X., Gu X., Li D., et al. (2025). Tertiary lymphoid structures as a biomarker in immunotherapy and beyond: Advancing towards clinical application. *Cancer Lett.* **613**:217491. DOI:10.1016/j.canlet.2025.217491
40. Sautès-Fridman C., Petitprez F., Calderaro J., et al. (2019). Tertiary lymphoid structures in the era of cancer immunotherapy. *Nat. Rev. Cancer* **19**:307–325. DOI:10.1038/s41568-019-0144-6
41. Le Rochais M., Ghamry-Barrin S., Panouillot M., et al. (2025). Imaging mass cytometry to decipher the maturation of tertiary lymphoid structures. *Methods Mol. Biol.* **2864**:159–179. DOI:10.1007/978-1-0716-4184-2_9
42. Hayashi Y., Makino T., Sato E., et al. (2023). Density and maturity of peritumoral tertiary lymphoid structures in oesophageal squamous cell carcinoma predicts patient survival and response to immune checkpoint inhibitors. *Br. J. Cancer* **128**:2175–2185. DOI:10.1038/s41416-023-02235-9
43. Song I.H., Heo S.-H., Bang W.S., et al. (2017). Predictive value of tertiary lymphoid structures assessed by high endothelial venule counts in the neoadjuvant setting of triple-negative breast cancer. *Cancer Res. Treat.* **49**:399–407. DOI:10.4143/crt.2016.215
44. Vanhersecke L., Bougouin A., Crombé A., et al. (2023). Standardized pathology screening of mature tertiary lymphoid structures in cancers. *Lab. Invest.* **103**:100063. DOI:10.1016/j.labinv.2023.100063
45. Germain C., Gnjatic S., Tamzalit F., et al. (2014). Presence of B cells in tertiary lymphoid structures is associated with a protective immunity in patients with lung cancer. *Am. J. Respir. Crit. Care Med.* **189**:832–844. DOI:10.1164/rccm.201309-1611OC
46. Siliņa K., Soltermann A., Attar F.M., et al. (2018). Germinal centers determine the prognostic relevance of tertiary lymphoid structures and are impaired by corticosteroids in lung squamous cell carcinoma. *Cancer Res.* **78**:1308–1320. DOI:10.1158/0008-5472.CAN-17-1987
47. Aoyama S., Noda T., Akita H., et al. (2025). Tumor-associated high endothelial venules are associated with enhanced lymphocyte infiltration and favorable prognosis in resected hepatocellular carcinoma. *Cancer Immunol. Immunother.* **75**:20. DOI:10.1007/s00262-025-04265-z
48. Posch F., Silina K., Leibl S., et al. (2018). Maturation of tertiary lymphoid structures and recurrence of stage II and III colorectal cancer. *OncoImmunology* **7**:e1378844. DOI:10.1080/2162402X.2017.1378844
49. Lynch K.T., Young S.J., Meneveau M.O., et al. (2021). Heterogeneity in tertiary lymphoid structure B-cells correlates with patient survival in metastatic melanoma. *J. Immunother. Cancer* **9**:e002273. DOI:10.1136/jitc-2020-002273
50. Werner F., Wagner C., Simon M., et al. (2021). A standardized analysis of tertiary lymphoid structures in human melanoma: Disease progression- and tumor site-associated changes with germinal center alteration. *Front. Immunol.* **12**:675146. DOI:10.3389/fimmu.2021.675146
51. Osorio J.C., Knorr D.A., Weitzenfeld P., et al. (2025). Fc-optimized CD40 agonistic antibody elicits tertiary lymphoid structure formation and systemic antitumor immunity in metastatic cancer. *Cancer Cell* **43**:1902–1916.e9. DOI:10.1016/j.ccell.2025.07.013
52. Gunderson A.J., Rajamanickam V., Bui C., et al. (2021). Germinal center reactions in tertiary lymphoid structures associate with neoantigen burden humoral immunity and long-term survivorship in pancreatic cancer. *OncoImmunology* **10**:1900635. DOI:10.1080/2162402X.2021.1900635
53. Sofopoulos M., Fortis S.P., Vaxevanis C.K., et al. (2019). The prognostic significance of peritumoral tertiary lymphoid structures in breast cancer. *Cancer Immunol. Immunother.* **68**:1733–1745. DOI:10.1007/s00262-019-02407-8
54. Fang Q., Chen S., Chen X., et al. (2025). Mature tertiary lymphoid structure associated CD103+ CD8+ trm cells determined improved anti-tumor immune in breast cancer. *Front. Oncol.* **15**:1480461. DOI:10.3389/fonc.2025.1480461
55. Li H., Liu H., Fu H., et al. (2021). Peritumoral tertiary lymphoid structures correlate with protective immunity and improved prognosis in patients with hepatocellular carcinoma. *Front. Immunol.* **12**:648812. DOI:10.3389/fimmu.2021.648812
56. Long S., Li M., Chen J., et al. (2024). Spatial patterns and MRI-based radiomic prediction of high peritumoral tertiary lymphoid structure density in hepatocellular carcinoma: A multicenter study. *J. Immunother. Cancer* **12**:e009879. DOI:10.1136/jitc-2024-009879
57. Li H., Wang J., Liu H., et al. (2020). Existence of intratumoral tertiary lymphoid structures is associated with immune cells infiltration and predicts better prognosis in early-stage hepatocellular carcinoma. *Aging* **12**:3451–3472. DOI:10.18632/aging.102821
58. Zhang T., Lei X., Jia W., et al. (2023). Peritumor tertiary lymphoid structures are associated with infiltrating neutrophils and inferior prognosis in hepatocellular carcinoma. *Cancer Med.* **12**:3068–3078. DOI:10.1002/cam4.5227
59. Finkin S., Yuan D., Stein I., et al. (2015). Ectopic lymphoid structures function as microniches for tumor progenitor cells in hepatocellular carcinoma. *Nat. Immunol.* **16**:1235–1244. DOI:10.1038/ni.3290
60. Calderaro J., Petitprez F., Becht E., et al. (2019). Intra-tumoral tertiary lymphoid structures are associated with a low risk of early recurrence of hepatocellular carcinoma. *J. Hepatol.* **70**:58–65. DOI:10.1016/j.jhep.2018.09.003
61. Li J., Zhang L., Xing H., et al. (2024). The absence of intra-tumoral tertiary lymphoid structures is associated with a worse prognosis and mtor signaling activation in hepatocellular carcinoma with liver transplantation: A multicenter retrospective study. *Adv. Sci.* **11**:e2309348. DOI:10.1002/advs.202309348
62. Xin S., Wen S., He P., et al. (2024). Density of tertiary lymphoid structures and their correlation with prognosis in non-small cell lung cancer. *Front. Immunol.* **15**:1423775. DOI:10.3389/fimmu.2024.1423775
63. Xu W., Lu J., Tian X., et al. (2024). Unveiling the impact of tertiary lymphoid structures on immunotherapeutic responses of clear cell renal cell carcinoma. *MedComm* **5**:e461. DOI:10.1002/mco2.461
64. Zhou C., Chen J., Wang Y., et al. (2026). Clinical and immunological significance of tertiary lymphoid structure maturation heterogeneity in brain metastases of lung adenocarcinoma. *J. Transl. Med.* **24**:396. DOI:10.1186/s12967-026-07852-5
65. Xu W., Lu J., Liu W.-R., et al. (2023). Heterogeneity in tertiary lymphoid structures predicts distinct prognosis and immune microenvironment characterizations of clear cell renal cell carcinoma. *J. Immunother. Cancer* **11**:e006667. DOI:10.1136/jitc-2023-006667
66. Deng M., Liu X., Jiang Y., et al. (2024). Tertiary lymphoid structures' pattern and prognostic value in primary adenocarcinoma of jejunum and ileum. *World J. Surg. Oncol.* **22**:261. DOI:10.1186/s12957-024-03543-x
67. Su G.-L., Zhang M.-J., Li H., et al. (2025). Dissecting tertiary lymphoid structures in cancer: Maturation, localization and density. *Theranostics* **15**:9459–9485. DOI:10.7150/thno.113940
68. Ding G.-Y., Ma J.-Q., Yun J.-P., et al. (2022). Distribution and density of tertiary lymphoid structures predict clinical outcome in intrahepatic cholangiocarcinoma. *J. Hepatol.* **76**:608–618. DOI:10.1016/j.jhep.2021.10.030
69. Elfving H., Yu H., Fessehatsion K.K., et al. (2025). Spatial distribution of tertiary lymphoid structures in the molecular and clinical context of non-small cell lung cancer. *Cell. Oncol.* **48**:801–813. DOI:10.1007/s13402-025-01052-x
70. Shu D.H., Ho W.J., Kagohara L.T., et al. (2024). Immunotherapy response induces divergent tertiary lymphoid structure morphologies in hepatocellular carcinoma. *Nat. Immunol.* **25**:2110–2123. DOI:10.1038/s41590-024-01992-w
71. Zhang C., Wang X.-Y., Zuo J.-L., et al. (2023). Localization and density of tertiary lymphoid structures associate with molecular subtype and clinical outcome in colorectal cancer liver metastases. *J. Immunother. Cancer* **11**:e006425. DOI:10.1136/jitc-2022-006425
72. Shang T., Jiang T., Lu T., et al. (2023). Tertiary lymphoid structures predict the prognosis and immunotherapy response of cholangiocarcinoma. *Front. Immunol.* **14**:1166497. DOI:10.3389/fimmu.2023.1166497
73. Cakmak P., Lun J.H., Singh A., et al. (2025). Spatial immune profiling defines a subset of human gliomas with functional tertiary lymphoid structures. *Immunity* **58**:2847–2863.e8. DOI:10.1016/j.immuni.2025.09.018
74. Tang Z., Bai Y., Fang Q., et al. (2025). Spatial transcriptomics reveals tryptophan metabolism restricting maturation of intratumoral tertiary lymphoid structures.

Cancer Cell **43**:1025–1044.e14. DOI:10.1016/j.ccell.2025.03.011
75. Du Bois H., Heim T.A. and Lund A.W. (2021). Tumor-draining lymph nodes: At the crossroads of metastasis and immunity. *Sci. Immunol.* **6**:eabg3551. DOI:10.1126/sciimmunol.abg3551
76. Zhu X., Maier G. and Panda S. (2024). Learning from circadian rhythm to transform cancer prevention prognosis and survivorship care. *Trends Cancer* **10**:196–207. DOI:10.1016/j.trecan.2023.11.002
77. Lanitis E., Irving M. and Coukos G. (2015). Targeting the tumor vasculature to enhance T cell activity. *Curr. Opin. Immunol.* **33**:55–63. DOI:10.1016/j.coi.2015.01.011
78. Thiemann S., Man J.H., Chang M.H., et al. (2015). Galectin-1 regulates tissue exit of specific dendritic cell populations. *J. Biol. Chem.* **290**:22662–22677. DOI:10.1074/jbc.M115.644799
79. Pietrobon V. and Marincola F.M. (2021). Hypoxia and the phenomenon of immune exclusion. *J. Transl. Med.* **19**:9. DOI:10.1186/s12967-020-02667-4
80. Geindreau M., Ghiringhelli F. and Bruchard M. (2021). Vascular endothelial growth factor, a key modulator of the anti-tumor immune response. *Int. J. Mol. Sci.* **22**:4871. DOI:10.3390/ijms22094871
81. Rodriguez A.B. and Engelhard V.H. (2020). Insights into tumor-associated tertiary lymphoid structures: Novel targets for antitumor immunity and cancer immunotherapy. *Cancer Immunol. Res.* **8**:1338–1345. DOI:10.1158/2326-6066.cir-20-0432
82. Asrir A., Tardiveau C., Coudert J., et al. (2022). Tumor-associated high endothelial venules mediate lymphocyte entry into tumors and predict response to PD-1 plus CTLA-4 combination immunotherapy. *Cancer Cell* **40**:318–334.e9. DOI:10.1016/j.ccell.2022.01.002
83. Li H., Zhang M.-J., Zhang B., et al. (2025). Mature tertiary lymphoid structures evoke intra-tumoral T and B cell responses via progenitor exhausted CD4+ T cells in head and neck cancer. *Nat. Commun.* **16**:4228. DOI:10.1038/s41467-025-59341-w
84. Kinker G.S., Vitiello G.A.F., Diniz A.B., et al. (2023). Mature tertiary lymphoid structures are key niches of tumour-specific immune responses in pancreatic ductal adenocarcinomas. *Gut* **72**:1927–1941. DOI:10.1136/gutjnl-2022-328697
85. Crotty S. (2011). Follicular helper CD4 T cells (T_{FH}). *Annu. Rev. Immunol.* **29**:621–663. DOI:10.1146/annurev-immunol-031210-101400
86. Esparcia-Pinedo L., Romero-Laorden N. and Alfranca, A. (2023). Tertiary lymphoid structures and B lymphocytes: A promising therapeutic strategy to fight cancer. *Front. Immunol.* **14**:1231315. DOI:10.3389/fimmu.2023.1231315
87. Vinuesa C.G., Linterman M.A., Yu D., et al. (2016). Follicular helper T cells. *Annu. Rev. Immunol.* **34**:335–368. DOI:10.1146/annurev-immunol-041015-055605
88. Bao X., Lin X., Xie M., et al. (2024). Mature tertiary lymphoid structures: Important contributors to anti-tumor immune efficacy. *Front. Immunol.* **15**:1413067. DOI:10.3389/fimmu.2024.1413067
89. Noël G., Fontsa M.L., Garaud S., et al. (2021). Functional Th1-oriented T follicular helper cells that infiltrate human breast cancer promote effective adaptive immunity. *J. Clin. Invest.* **131**:e139905. DOI:10.1172/JCI139905
90. Ukita M., Hamanishi J., Yoshitomi H., et al. (2022). CXCL13-producing $CD4^+$ T cells accumulate in the early phase of tertiary lymphoid structures in ovarian cancer. *JCI Insight* **7**:e157215. DOI:10.1172/jci.insight.157215
91. Li J.-P., Wu C.-Y., Chen M.-Y., et al. (2021). PD-1+CXCR5-CD4+ Th-CXCL13 cell subset drives B cells into tertiary lymphoid structures of nasopharyngeal carcinoma. *J. Immunother. Cancer* **9**:e002101. DOI:10.1136/jitc-2020-002101
92. Im S.J., Obeng R.C., Nasti T.H., et al. (2023). Characteristics and anatomic location of PD-1+TCF1+ stem-like CD8 T cells in chronic viral infection and cancer. *Proc. Natl. Acad. Sci. USA.* **120**:e2221985120. DOI:10.1073/pnas.2221985120
93. Tanoue K., Ohmura H., Uehara K., et al. (2024). Spatial dynamics of CD39+CD8+ exhausted T cell reveal tertiary lymphoid structures-mediated response to PD-1 blockade in esophageal cancer. *Nat. Commun.* **15**:9033. DOI:10.1038/s41467-024-53262-w
94. Tran K., Kumari A.N., Raghu D., et al. (2024). T cell factor 1 (TCF-1) defines T cell differentiation in colorectal cancer. *iScience* **27**:110754. DOI:10.1016/j.isci.2024.110754
95. Im S.J., Hashimoto M., Gerner M.Y., et al. (2016). Defining CD8+ T cells that provide the proliferative burst after PD-1 therapy. *Nature* **537**:417–421. DOI:10.1038/nature19330
96. Siddiqui I., Schaeuble K., Chennupati V., et al. (2019). Intratumoral Tcf1+PD-1+CD8+ T cells with stem-like properties promote tumor control in response to vaccination and checkpoint blockade immunotherapy. *Immunity* **50**:195–211.e10. DOI:10.1016/j.immuni.2018.12.021
97. Miller B.C., Sen D.R., Al Abosy R., et al. (2019). Subsets of exhausted CD8+ T cells differentially mediate tumor control and respond to checkpoint blockade. *Nat. Immunol.* **20**:326–336. DOI:10.1038/s41590-019-0312-6
98. Schenkel J.M., Herbst R.H., Canner D., et al. (2021). Conventional type I dendritic cells maintain a reservoir of proliferative tumor-antigen specific TCF-1+ CD8+ T cells in tumor-draining lymph nodes. *Immunity* **54**:2338–2353.e6. DOI:10.1016/j.immuni.2021.08.026
99. Kasikova L., Rakova J., Hensler M., et al. (2024). Tertiary lymphoid structures and B cells determine clinically relevant T cell phenotypes in ovarian cancer. *Nat. Commun.* **15**:2528. DOI:10.1038/s41467-024-46873-w
100. Joshi N.S., Akama-Garren E.H., Lu Y., et al. (2015). Regulatory T cells in tumor-associated tertiary lymphoid structures suppress anti-tumor T cell responses. *Immunity* **43**:579–590. DOI:10.1016/j.immuni.2015.08.006
101. Devi-Marulkar P., Fastenackels S., Karapentiantz P., et al. (2022). Regulatory T cells infiltrate the tumor-induced tertiary lymphoïd structures and are associated with poor clinical outcome in NSCLC. *Commun. Biol.* **5**:1416. DOI:10.1038/s42003-022-04356-y
102. Davies A.M. and Sutton B.J. (2015). Human IgG4: A structural perspective. *Immunol. Rev.* **268**:139–159. DOI:10.1111/imr.12349
103. Wang H., Li J., Wang Y., et al. (2025). IgG4-mediated M2 macrophage polarization in tertiary lymphoid structures of esophageal cancer: Implications for immunosuppression. *Front. Immunol.* **15**:1497783. DOI:10.3389/fimmu.2024.1497783
104. Su C., Chen S., He X., et al. (2025). Increased IgG4 expression within tertiary lymphoid structures of esophageal cancer and implications for prognosis. *Front. Immunol.* **16**:1654655. DOI:10.3389/fimmu.2025.1654655
105. Chen C., An M., Zheng H., et al. (2026). B cells disrupt tertiary lymphoid structure formation and suppress anti-tumor immunity. *Cancer Cell* **44**:551–566.e17. DOI:10.1016/j.ccell.2025.12.011
106. Huang Q., Wang F., Li X., et al. (2025). Multi-omics profiling reveals an immunosuppressive plasma cell subset within tertiary lymphoid structures in cervical cancer. *Cancer Immunol. Immunother.* **75**:26. DOI:10.1007/s00262-025-04268-w
107. Meylan M., Petitprez F., Becht E., et al. (2022). Tertiary lymphoid structures generate and propagate anti-tumor antibody-producing plasma cells in renal cell cancer. *Immunity* **55**:527–541.e5. DOI:10.1016/j.immuni.2022.02.001
108. Lehmann J., Thelen M., Kreer C., et al. (2024). Tertiary lymphoid structures in pancreatic cancer are structurally homologous, share gene expression patterns and B-cell clones with secondary lymphoid organs but show increased T-cell activation. *Cancer Immunol. Res.* **13**:323–336. DOI:10.1158/2326-6066.cir-24-0299
109. He M., He Q., Cai X., et al. (2023). Intratumoral tertiary lymphoid structure (TLS) maturation is influenced by draining lymph nodes of lung cancer. *J. Immunother. Cancer* **11**:e005539. DOI:10.1136/jitc-2022-005539
110. Gao J., Gu D., Yang K., et al. (2025). Infiltrating plasma cells maintain glioblastoma stem cells through IgG-tumor binding. *Cancer Cell* **43**:122–143.e8. DOI:10.1016/j.ccell.2024.12.006
111. Sammut S.-J., Galson J.D., Minter R., et al. (2024). Predictability of B cell clonal persistence and immunosurveillance in breast cancer. *Nat. Immunol.* **25**:916–924. DOI:10.1038/s41590-024-01821-0
112. Che Y., Lee J., Abou-Taleb F., et al. (2025). Induced B cell receptor diversity predicts PD-1 blockade immunotherapy response. *Proc. Natl. Acad. Sci. USA* **122**:e2501269122. DOI:10.1073/pnas.2501269122
113. Goc J., Germain C., Vo-Bourgais T.K.D., et al. (2014). Dendritic cells in tumor-associated tertiary lymphoid structures signal a Th1 cytotoxic immune contexture and license the positive prognostic value of infiltrating CD8+ T cells. *Cancer Res.* **74**:705–715. DOI:10.1158/0008-5472.CAN-13-1342
114. Berthe J., Poudel P., Segerer F.J., et al. (2024). Exploring the impact of tertiary lymphoid structures maturity in NSCLC: Insights from TLS scoring. *Front. Immunol.* **15**:1422206. DOI:10.3389/fimmu.2024.1422206
115. Wang M., Shi J., Xu K., et al. (2026). T cell exhaustion and dendritic cell-mediated tertiary lymphoid structures (TLSs) modulation affect response to neoadjuvant chemoradiotherapy in microsatellite stable rectal cancer. *Adv. Sci.* **13**:e14332. DOI:10.1002/advs.202514332
116. Syding L.A., Plačková K., Pavelková L., et al. (2025). High treg and PMN-MDSC densities are a hallmark of tertiary lymphoid structures in fatal cases of cervical cancer. *J. Immunother. Cancer* **13**:e012613. DOI:10.1136/jitc-2025-012613
117. Condamine T., Dominguez G.A., Youn J.-I., et al. (2016). Lectin-type oxidized LDL receptor-1 distinguishes population of human polymorphonuclear myeloid-derived suppressor cells in cancer patients. *Sci. Immunol.* **1**:aaf8943–aaf8943. DOI:10.1126/sciimmunol.aaf8943
118. Zhao F., Hoechst B., Duffy A., et al. (2012). A9 a new marker for monocytic human myeloid - derived suppressor cells. *Immunology* **136**:176–183. DOI:10.1111/j.1365-2567.2012.03566.x
119. Lesokhin A.M., Hohl T.M., Kitano S., et al. (2012). Monocytic CCR2+ myeloid-derived suppressor cells promote immune escape by limiting activated CD8 T-cell infiltration into the tumor microenvironment. *Cancer Res.* **72**:876–886. DOI:10.1158/0008-5472.CAN-11-1792
120. Groth C., Hu X., Weber R., et al. (2019). Immunosuppression mediated by myeloid-derived suppressor cells (MDSCs) during tumour progression. *Br. J. Cancer* **120**:16–25. DOI:10.1038/s41416-018-0333-1
121. Rodríguez P.C. and Ochoa A.C. (2008). Arginine regulation by myeloid derived suppressor cells and tolerance in cancer: Mechanisms and therapeutic perspectives. *Immunol. Rev.* **222**:180–191. DOI:10.1111/j.1600-065X.2008.00608.x
122. Baniyash M. (2004). TCR ζ-chain downregulation: Curtailing an excessive inflammatory immune response. *Nat. Rev. Immunol.* **4**:675–687. DOI:10.1038/nri1434
123. Kittang A.O., Kordasti S., Sand K.E., et al. (2016). Expansion of myeloid derived suppressor cells correlates with number of T regulatory cells and disease

progression in myelodysplastic syndrome. *OncoImmunology* **5**:e1062208. DOI:10.1080/2162402X.2015.1062208
124. Marcovecchio P.M., Thomas G. and Salek-Ardakani S. (2021). CXCL9-expressing tumor-associated macrophages: New players in the fight against cancer. *J. Immunother. Cancer* **9**:e002045. DOI:10.1136/jitc-2020-002045
125. Duan Z. and Luo Y. (2021). Targeting macrophages in cancer immunotherapy. *Signal Transduct. Target. Ther.* **6**:127. DOI:10.1038/s41392-021-00506-6
126. Guedj K., Khallou-Laschet J., Clement M., et al. (2014). M1 macrophages act as LTβR-independent lymphoid tissue inducer cells during atherosclerosis-related lymphoid neogenesis. *Cardiovasc. Res.* **101**:434–443. DOI:10.1093/cvr/cvt263
127. Labadie B.W.,Bao R. and Luke J.J. (2019). Reimagining IDO pathway inhibition in cancer immunotherapy via downstream focus on the tryptophan–kynurenine–aryl hydrocarbon axis. *Clin. Cancer Res.* **25**:1462–1471. DOI:10.1158/1078-0432.CCR-18-2882
128. Laviron M., Petit M., Weber-Delacroix E., et al. (2022). Tumor-associated macrophage heterogeneity is driven by tissue territories in breast cancer. *Cell Rep.* **39**:110865. DOI:10.1016/j.celrep.2022.110865
129. Ma R.-Y., Black A. and Qian B.-Z. (2022). Macrophage diversity in cancer revisited in the era of single-cell omics. *Trends Immunol.* **43**:546–563. DOI:10.1016/j.it.2022.04.008
130. Sica A., Larghi P., Mancino A., et al. (2008). Macrophage polarization in tumour progression. *Semin. Cancer Biol.* **18**:349–355. DOI:10.1016/j.semcancer.2008.03.004
131. Xu R., Liu H., Zhu T., et al. (2025). An immunosuppressive tertiary lymphoid structure is associated with adverse prognosis in gastric-type endocervical adenocarcinoma. *J. Natl. Cancer Inst.* **118**:276–288. DOI:10.1093/jnci/djaf310
132. Petroni G., Scolari F., Scoccianti G., et al. (2025). Th17-like cells and immunosuppressive macrophages infiltrate tertiary lymphoid structures with distinct maturation status in soft-tissue sarcoma. *Cell Death Dis.* **16**:917. DOI:10.1038/s41419-025-08376-4
133. Sánchez-Alonso S., Setti-Jerez G., Arroyo M., et al. (2020). A new role for circulating T follicular helper cells in humoral response to anti-PD-1 therapy. *J. Immunother. Cancer* **8**:e001187. DOI:10.1136/jitc-2020-001187
134. Matsumoto K., Noda Y., Hachiya K., et al. (2026). Single-cell spatial analysis identifies ID1-high endothelial cells in tertiary lymphoid structures as predictors of durable response to immunotherapy in non-small cell lung cancer. *Cancer Cell Int.* **26**:65. DOI:10.1186/s12935-025-04161-7
135. Liu S.-X., Wu T.-W., Luo D.-H., et al. (2025). 26 Interferon-responsive HEVs drive tumor tertiary lymphoid structure formation and predict immunotherapy response in nasopharyngeal carcinoma. *Cell Rep. Med.* **6**:102200. DOI:10.1016/j.xcrm.2025.102200
136. Onder L., Papadopoulou C., Lütge A., et al. (2025). Fibroblastic reticular cells generate protective intratumoral T cell environments in lung cancer. *Cell* **188**:430–446.e20. DOI:10.1016/j.cell.2024.10.042
137. Peyraud F., Guégan J.-P., Rey C., et al. (2025). Spatially resolved transcriptomics reveal the determinants of primary resistance to immunotherapy in NSCLC with mature tertiary lymphoid structures. *Cell Rep. Med.* **6**:101934. DOI:10.1016/j.xcrm.2025.101934
138. O'Connor R.A., Martinez B.R., Koppensteiner L., et al. (2023). Cancer-associated fibroblasts drive CXCL13 production in activated T cells via TGF-beta. *Front. Immunol.* **14**:1221532. DOI:10.3389/fimmu.2023.1221532
139. Morcrette G., Hirsch T.Z., Badour E., et al. (2019). APC germline hepatoblastomas demonstrate cisplatin-induced intratumor tertiary lymphoid structures. *OncoImmunology* **8**:e1583547. DOI:10.1080/2162402X.2019.1583547
140. Lanickova T., Hensler M., Kasikova L., et al. (2025). Chemotherapy drives tertiary lymphoid structures that correlate with ICI-responsive TCF1+CD8+ T cells in metastatic ovarian cancer. *Clin. Cancer Res.* **31**:164–180. DOI:10.1158/1078-0432.CCR-24-1594
141. Lv J., Wei Y., Yin J.-H., et al. (2023). The tumor immune microenvironment of nasopharyngeal carcinoma after gemcitabine plus cisplatin treatment. *Nat. Med.* **29**:1424–1436. DOI:10.1038/s41591-023-02369-6
142. Tian N., Wang Q., Lv Y., et al. (2025). Mature tertiary lymphoid structures support B cell-mediated antitumour immunity and are disrupted by neoadjuvant therapy in rectal cancer: A multicentre retrospective study. *eBioMedicine* **122**:106030. DOI:10.1016/j.ebiom.2025.106030
143. Constantinides A., Lansu N., Mosen P., et al. (2025). Treatment of colorectal peritoneal metastases with oxaliplatin induces biomarkers predicting response to immune checkpoint blockade. *Transl. Oncol.* **59**:102464. DOI:10.1016/j.tranon.2025.102464
144. Xing R., Mei J., Zuo Z., et al. (2025). Enhanced formation of tertiary lymphoid structures shapes the anti-tumor microenvironment in hepatocellular carcinoma after FOLFOX-HAIC therapy. *Cell Rep. Med.* **6**:102298. DOI:10.1016/j.xcrm.2025.102298
145. Huang Y., Du Z., Lai Z., et al. (2025). Single-nucleus and spatial transcriptome profiling delineates the multicellular ecosystem in hepatocellular carcinoma after hepatic arterial infusion chemotherapy. *Adv. Sci.* **12**:2405749. DOI:10.1002/advs.202405749
146. Rupp L., Dietsche I., Kießler M., et al. (2024). Neoadjuvant chemotherapy is associated with suppression of the B cell-centered immune landscape in pancreatic ductal adenocarcinoma. *Front. Immunol.* **15**:1378190. DOI:10.3389/fimmu.2024.1378190
147. Delvecchio F.R., Fincham R.E.A., Spear S., et al. (2021). Pancreatic cancer chemotherapy is potentiated by induction of tertiary lymphoid structures in mice. *Cell. Mol. Gastroenterol. Hepatol.* **12**:1543–1565. DOI:10.1016/j.jcmgh.2021.06.023
148. Fucikova J., Kepp O., Kasikova L., et al. (2020). Detection of immunogenic cell death and its relevance for cancer therapy. *Cell Death Dis.* **11**:1013. DOI:10.1038/s41419-020-03221-2
149. Adkins I., Fucikova J., Garg A.D., et al. (2015). Physical modalities inducing immunogenic tumor cell death for cancer immunotherapy. *OncoImmunology* **3**:e968434. DOI:10.4161/21624011.2014.968434
150. Zhao H., Zhao Y., Zhang S., et al. (2024). Effects of immunogenic cell death-inducing chemotherapeutics on the immune cell activation and tertiary lymphoid structure formation in melanoma. *Front. Immunol.* **15**:1302751. DOI:10.3389/fimmu.2024.1302751
151. Bertucci F., De Nonneville A., Finetti P., et al. (2023). Predictive power of tertiary lymphoid structure signature for neoadjuvant chemotherapy response and immunotherapy benefit in HER2 - negative breast cancer. *Cancer Commun.* **43**:943–946. DOI:10.1002/cac2.12447
152. Wei Z., Lin K., Deng W., et al. (2025). Tertiary lymphoid structures are associated with lower axillary residual nodal burden in breast cancer patients after neoadjuvant chemotherapy. *Eur. J. Med. Res.* **30**:1263. DOI:10.1186/s40001-025-03556-6
153. Cabrero-de las Heras S., Hernández-Yagüe X., González A., et al. (2024). Changes In serum CXCL13 levels are associated with outcomes of colorectal cancer patients undergoing first-line oxaliplatin-based treatment. *Biomed. Pharmacother.* **176**:116857. DOI:10.1016/j.biopha.2024.116857
154. Benzerdjeb N., Dartigues P., Kepenekian V., et al. (2021). Tertiary lymphoid structures in epithelioid malignant peritoneal mesothelioma are associated with neoadjuvant chemotherapy but not with prognosis. *Virchows Arch.* **479**:765–772. DOI:10.1007/s00428-021-03099-1
155. Li S., Chen K., Sun Z., et al. (2024). Radiation drives tertiary lymphoid structures to reshape TME for synergized antitumour immunity. *Expert Rev. Mol. Med.* **26**:e30. DOI:10.1017/erm.2024.27
156. Boivin G., Kalambaden P., Faget J., et al. (2018). Cellular composition and contribution of tertiary lymphoid structures to tumor immune infiltration and modulation by radiation therapy. *Front. Oncol.* **8**:256. DOI:10.3389/fonc.2018.00256
157. Mills B.N., Qiu H., Drage M.G., et al. (2022). Modulation of the human pancreatic ductal adenocarcinoma immune microenvironment by stereotactic body radiotherapy. *Clin. Cancer Res.* **28**:150–162. DOI:10.1158/1078-0432.CCR-21-2495
158. Wang Q., Zhong W., Shen X., et al. (2024). Tertiary lymphoid structures predict survival and response to neoadjuvant therapy in locally advanced rectal cancer. *Npj Precis. Oncol.* **8**:61. DOI:10.1038/s41698-024-00533-w
159. Huang H., Zhao G., Wang T., et al. (2024). Survival benefit and spatial properties of tertiary lymphoid structures in esophageal squamous cell carcinoma with neoadjuvant therapies. *Cancer Lett.* **601**:217178. DOI:10.1016/j.canlet.2024.217178
160. Wang D., Huang L., Qian D., et al. (2023). Low-dose radiotherapy promotes the formation of tertiary lymphoid structures in lung adenocarcinoma. *Front. Immunol.* **14**:1334408. DOI:10.3389/fimmu.2023.1334408
161. Zhai K., Xie R., Ru K., et al. (2025). Tertiary lymphoid structures correlate with the therapeutic efficacy and prognosis of resectable esophageal squamous cell carcinoma undergoing neoadjuvant chemoradiotherapy plus immunotherapy. *Front. Immunol.* **16**:1616247. DOI:10.3389/fimmu.2025.1616247
162. Huang J., Theelen W.S.M.E., Belcaid Z., et al. (2025). Combination of pembrolizumab and radiotherapy induces systemic antitumor immune responses in immunologically cold non-small cell lung cancer. *Nat. Cancer* **6**:1676–1692. DOI:10.1038/s43018-025-01018-w
163. Huang Y.-S., Li Z., Xiao Z.-F., et al. (2022). Case report: Radiotherapy plus pneumococcal conjugate vaccine stimulates abscopal immune response in a patient with ALK+ NSCLC. *Front. Immunol.* **13**:950252. DOI:10.3389/fimmu.2022.950252
164. Shiao S.L., Gouin K.H., Ing N., et al. (2024). Single-cell and spatial profiling identify three response trajectories to pembrolizumab and radiation therapy in triple negative breast cancer. *Cancer Cell* **42**:70–84.e8. DOI:10.1016/j.ccell.2023.12.012
165. van Hooren L., Handgraaf S.M., Kloosterman D.J., et al. (2023). CD103+ regulatory T cells underlie resistance to radio-immunotherapy and impair CD8+ T cell activation in glioblastoma. *Nat. Cancer* **4**:665–681. DOI:10.1038/s43018-023-00547-6
166. Deng L., Liang H., Xu M., et al. (2014). STING-dependent cytosolic DNA sensing promotes radiation-induced type I interferon-dependent antitumor immunity in immunogenic tumors. *Immunity* **41**:843–852. DOI:10.1016/j.immuni.2014.10.019
167. Vanpouille-Box C., Alard A., Aryankalayil M.J., et al. (2017). DNA exonuclease Trex1 regulates radiotherapy-induced tumour immunogenicity. *Nat. Commun.* **8**:15618. DOI:10.1038/ncomms15618
168. Herrera F.G., Ronet C., Ochoa de Olza M., et al. (2022). Low-dose radiotherapy reverses tumor immune desertification and resistance to immunotherapy. *Cancer Discov.* **12**:108–133. DOI:10.1158/2159-8290.CD-21-0003
169. Italiano A., Bessede A., Pulido M., et al. (2022). Pembrolizumab in soft-tissue sarcomas with tertiary lymphoid structures: A phase 2 PEMBROSARC trial cohort.

Nat. Med. **28**:1199–1206. DOI:10.1038/s41591-022-01821-3
170. Chung S.-Y., Yeh Y.-C., Huang C.-J., et al. (2025). Comparative impact of tertiary lymphoid structures and tumor-infiltrating lymphocytes in cholangiocarcinoma. *J. Immunother. Cancer* **13**:e010173. DOI:10.1136/jitc-2024-010173
171. Sadeghirad H., Monkman J., Tan C.W., et al. (2024). Spatial dynamics of tertiary lymphoid aggregates in head and neck cancer: Insights into immunotherapy response. *J. Transl. Med.* **22**:677. DOI:10.1186/s12967-024-05409-y
172. Xie Y., Peng H., Hu Y., et al. (2025). Immune microenvironment spatial landscapes of tertiary lymphoid structures in gastric cancer. *BMC Med.* **23**:59. DOI:10.1186/s12916-025-03889-3
173. Vanhersecke L., Brunet M., Guégan J.-P., et al. (2021). Mature tertiary lymphoid structures predict immune checkpoint inhibitor efficacy in solid tumors independently of PD-L1 expression. *Nat. Cancer* **2**:794–802. DOI:10.1038/s43018-021-00232-6
174. van Hooren L., Vaccaro A., Ramachandran, M., et al. (2021). Agonistic CD40 therapy induces tertiary lymphoid structures but impairs responses to checkpoint blockade in glioma. *Nat. Commun.* **12**:4127. DOI:10.1038/s41467-021-24347-7
175. Levy A., Morel D., Texier M., et al. (2025). Monocyte-lineage tumor infiltration predicts immunoradiotherapy response in advanced pretreated soft-tissue sarcoma: Phase 2 trial results. *Signal Transduct. Target. Ther.* **10**:103. DOI:10.1038/s41392-025-02173-3
176. Hua Y., Vella G., Rambow F., et al. (2022). Cancer immunotherapies transition endothelial cells into high-endothelial venules that generate TCF1+ T lymphocyte niches through a feed-forward loop. *Cancer Cell* **40**:1600–1618.e10. DOI:10.1016/j.ccell.2022.11.002
177. Eschweiler S., Clarke J., Ramírez-Suástegui C., et al. (2021). Intratumoral follicular regulatory T cells curtail anti-PD-1 treatment efficacy. *Nat. Immunol.* **22**:1052–1063. DOI:10.1038/s41590-021-00958-6
178. Cheng R., Li S., Ma X., et al. (2025). Intratumoral antigen-presenting cell activation by a nanovesicle for the concurrent tertiary lymphoid structure de novo neogenesis. *Sci. Adv.* **11**:eadr1299. DOI:10.1126/sciadv.adr1299
179. Ahn W., Han J., Kim N., et al. (2025). Hierarchical protein nano-crystalline hydrogel with extracellular vesicles for ectopic lymphoid structure formation. *Biomaterials* **318**:123166. DOI:10.1016/j.biomaterials.2025.123166
180. Mi Z., Chen J., Zhang Z., et al. (2025). Synthetic biology–driven induction of mature TLS formation enhances antitumor immunity in colorectal cancer. *Sci. Transl. Med.* **17**:eado8395. DOI:10.1126/scitranslmed.ado8395
181. Ramachandran M., Vaccaro A., Van De Walle T., et al. (2023). Tailoring vascular phenotype through AAV therapy promotes anti-tumor immunity in glioma. *Cancer Cell* **41**:1134–1151.e10. DOI:10.1016/j.ccell.2023.04.010
182. Kuwentrai C., Tang W., Lin X., et al. (2025). Injectable hydrogel-based drug formulation for enhancing tertiary lymphoid structure formation and cancer immunotherapy efficacy. *J. Controlled Release* **384**:113897. DOI:10.1016/j.jconrel.2025.113897
183. Falahat R. and Mulé J.J. (2025). Chemokine/cytokine-releasing biomaterials induce in situ tertiary lymphoid-like structures and enhance antitumor immunity. *Proc. Natl. Acad. Sci. USA* **122**:e2409560122. DOI:10.1073/pnas.2409560122
184. Kuang G., Zhang Q., Li W., et al. (2024). Biomimetic tertiary lymphoid structures with microporous annealed particle scaffolds for cancer postoperative therapy. *ACS Nano* **18**:9176–9186. DOI:10.1021/acsnano.4c01180
185. Zhang L., Zhang B., Zhang M.-J., et al. (2025). Trigger inducible tertiary lymphoid structure formation using covalent organic frameworks for cancer immunotherapy. *Nat. Commun.* **16**:44. DOI:10.1038/s41467-024-55430-4
186. Yang Q.-C., Wang Y.-Y., Wang S., et al. (2025). Engineered bacterial membrane biomimetic covalent organic framework as nano-immunopotentiator for cancer immunotherapy. *Bioact. Mater.* **47**:283–294. DOI:10.1016/j.bioactmat.2025.01.018
187. Wang F., Zeng Y., Yan M., et al. (2026). Self-transforming hydrogel mimicking tertiary lymph nodes to activate cGAS-STING pathway for enhanced antitumor immunotherapy. *Sci. Adv.* **12**:eadz5078. DOI:10.1126/sciadv.adz5078
188. Li M., Lu L., Bao Q., et al. (2025). Radiotherapy-derived engineered stem cell exosomes improve anti-glioma immunotherapy by promoting the formation of tertiary lymphoid structure and improve the release of type I interferon. *J. Nanobiotechnology* **23**:239. DOI:10.1186/s12951-025-03301-5
189. Zhang M.-J., Lin W.-P., Wang Q., et al. (2025). Oncolytic herpes simplex virus propagates tertiary lymphoid structure formation via CXCL10/CXCR3 to boost antitumor immunity. *Cell Prolif.* **58**:e13740. DOI:10.1111/cpr.13740
190. He T., Hao Z., Lin M., et al. (2022). Oncolytic adenovirus promotes vascular normalization and nonclassical tertiary lymphoid structure formation through STING-mediated DC activation. *OncoImmunology* **11**:2093054. DOI:10.1080/2162402X.2022.2093054
191. Hu L., Li T., Deng S., et al. (2025). Tertiary lymphoid structure formation induced by LIGHT-engineered and photosensitive nanoparticles-decorated bacteria enhances immune response against colorectal cancer. *Biomaterials* **314**:122846. DOI:10.1016/j.biomaterials.2024.122846
192. Zhang N., Liu X., Qin J., et al. (2023). LIGHT/TNFSF14 promotes CAR-T cell trafficking and cytotoxicity through reversing immunosuppressive tumor microenvironment. *Mol. Ther.* **31**:2575–2590. DOI:10.1016/j.ymthe.2023.06.015
193. Li C., Clauson R., Bugada L.F., et al. (2024). Antigen-clustered nanovaccine achieves long-term tumor remission by promoting B/CD 4 T cell crosstalk. *ACS Nano* **18**:9584–9604. DOI:10.1021/acsnano.3c13038
194. Wen Z., Liu H., Qiao D., et al. (2023). Nanovaccines fostering tertiary lymphoid structure to attack mimicry nasopharyngeal carcinoma. *ACS Nano* **17**:7194–7206. DOI:10.1021/acsnano.2c09619
195. Chen G., Li T., Duan R., et al. (2025). Cognate nanovaccine promotes tertiary lymphoid structures function and strengthens immune cell cross-talk by targeting exhausted T cells in nonimmunogenic cancers. *ACS Nano* **19**:21385–21399. DOI:10.1021/acsnano.5c01280
196. Yang X., Jiang S., Liu F., et al. (2024). HCMV IE1/IE1mut therapeutic vaccine induces tumor regression via intratumoral tertiary lymphoid structure formation and peripheral immunity activation in glioblastoma multiforme. *Mol. Neurobiol.* **61**:5935–5949. DOI:10.1007/s12035-024-03937-8
197. Zhang Y., Xu J., Fei Z., et al. (2021). 3D printing scaffold vaccine for antitumor immunity. *Adv. Mater.* **33**:2106768. DOI:10.1002/adma.202106768
198. Aeffner F., Zarella M.D., Buchbinder N., et al. (2019). Introduction to digital image analysis in whole-slide imaging: A white paper from the digital pathology association. *J. Pathol. Inform.* **10**:9. DOI:10.4103/jpi.jpi_82_18
199. Abels E., Pantanowitz L., Aeffner F., et al. (2019). Computational pathology definitions, best practices, and recommendations for regulatory guidance: A white paper from the digital pathology association. *J. Pathol.* **249**:286–294. DOI:10.1002/path.5331
200. van Rijthoven M., Obahor S., Pagliarulo F., et al. (2024). Multi-resolution deep learning characterizes tertiary lymphoid structures and their prognostic relevance in solid tumors. *Commun. Med.* **4**:5. DOI:10.1038/s43856-023-00421-7
201. Chen Y., Sun Z., Yin J., et al. (2024). Digital assessment of tertiary lymphoid structures and therapeutic responses in gastric cancer: A multicentric retrospective study. *Int. J. Surg.* **110**:6732–6747. DOI:10.1097/JS9.0000000000001834
202. Zhao Z., Chen D., Wang R., et al. (2026). Multiview deep-learning-enabled histopathology for prognostic and therapeutic stratification in stage II colorectal cancer: A retrospective multicenter study. *PLOS Med.* **23**:e1004614. DOI:10.1371/journal.pmed.1004614
203. Le Rochais M., Brahim I., Zeghlache R., et al. (2025). Automated classification of tertiary lymphoid structures in colorectal cancer using TLS-PAT artificial intelligence tool. *Sci. Rep.* **15**:9845. DOI:10.1038/s41598-025-94664-0
204. Suzuki H., Hamada K., Hamanishi J., et al. (2025). Artificial intelligence-based spatial analysis of tertiary lymphoid structures and clinical significance for endometrial cancer. *Cancer Immunol. Immunother.* **74**:84. DOI:10.1007/s00262-024-03929-6
205. Xia P., Chen D., An H., et al. (2025). Learnable prototype-guided multiple instance learning for detecting tertiary lymphoid structures in multi-cancer whole-slide pathological images. *Med. Image Anal.* **104**:103652. DOI:10.1016/j.media.2025.103652
206. Messina J.L., Fenstermacher D.A., Eschrich S., et al. (2012). 12-chemokine gene signature identifies lymph node-like structures in melanoma: Potential for patient selection for immunotherapy. *Sci. Rep.* **2**:765. DOI:10.1038/srep00765
207. Tokunaga R., Nakagawa S., Sakamoto Y., et al. (2020). 12 - chemokine signature a predictor of tumor recurrence in colorectal cancer. *Int. J. Cancer* **147**:532–541. DOI:10.1002/ijc.32982
208. Li R., Berglund A., Zemp L., et al. (2021). The 12-CK score: Global measurement of tertiary lymphoid structures. *Front. Immunol.* **12**:694079. DOI:10.3389/fimmu.2021.694079
209. Li K., Guo Q., Zhang X., et al. (2020). Oral cancer-associated tertiary lymphoid structures: Gene expression profile and prognostic value. *Clin. Exp. Immunol.* **199**:172–181. DOI:10.1111/cei.13389
210. Hou Y., Qiao S., Li M., et al. (2023). The gene signature of tertiary lymphoid structures within ovarian cancer predicts the prognosis and immunotherapy benefit. *Front. Genet.* **13**:1090640. DOI:10.3389/fgene.2022.1090640
211. Wang X., Venet D., Lifrange F., et al. (2024). Spatial transcriptomics reveals substantial heterogeneity in triple-negative breast cancer with potential clinical implications. *Nat. Commun.* **15**:10232. DOI:10.1038/s41467-024-54145-w
212. MacFawn I.P., Magnon G., Gorecki G., et al. (2024). The activity of tertiary lymphoid structures in high grade serous ovarian cancer is governed by site, stroma, and cellular interactions. *Cancer Cell* **42**:1864–1881.e5. DOI:10.1016/j.ccell.2024.09.007
213. Zhang Y., Yu B., Ming W., et al. (2024). SpaTopic: A statistical learning framework for exploring tumor spatial architecture from spatially resolved transcriptomic data. *Sci. Adv.* **10**:eadp4942. DOI:10.1126/sciadv.adp4942
214. Lin J., Jiang S., Chen B., et al. (2025). Tertiary lymphoid structures are linked to enhanced antitumor immunity and better prognosis in muscle - invasive bladder cancer. *Adv. Sci.* **12**:2410998. DOI:10.1002/advs.202410998
215. Groeneveld C.S., Fontugne J., Cabel L., et al. (2021). Tertiary lymphoid structures marker CXCL13 is associated with better survival for patients with advanced-stage bladder cancer treated with immunotherapy. *Eur. J. Cancer* **148**:181–189. DOI:10.1016/j.ejca.2021.01.036
216. Du W., Xiao B., Yang X., et al. (2025). Tertiary lymphoid structures gene signature predicts response to immunotherapy plus chemotherapy in advanced non-small cell lung cancer. *Cancer Immunol. Immunother.* **74**:307. DOI:10.1007/s00262-025-04165-2
217. Sala E., Mema E., Himoto Y., et al. (2017). Unravelling tumour heterogeneity using

next-generation imaging: Radiomics, radiogenomics, and habitat imaging. *Clin. Radiol.* **72**:3–10. DOI:10.1016/j.crad.2016.09.013
218. Lambin P., Leijenaar R.T.H., Deist T.M., et al. (2017). Radiomics: The bridge between medical imaging and personalized medicine. *Nat. Rev. Clin. Oncol.* **14**:749–762. DOI:10.1038/nrclinonc.2017.141
219. Sun R., Henry T., Laville A., et al. (2022). Imaging approaches and radiomics: Toward a new era of ultraprecision radioimmunotherapy. *J. Immunother. Cancer* **10**:e004848. DOI:10.1136/jitc-2022-004848
220. Zhao X., Wang Y., Xue M., et al. (2024). Preoperative assessment of tertiary lymphoid structures in stage I lung adenocarcinoma using CT radiomics: A multicenter retrospective cohort study. *Cancer Imaging* **24**:167. DOI:10.1186/s40644-024-00813-5
221. Xu Y., Li Z., Yang Y., et al. (2023). A CT-based radiomics approach to predict intratumoral tertiary lymphoid structures and recurrence of intrahepatic cholangiocarcinoma. *Insights Imaging* **14**:173. DOI:10.1186/s13244-023-01527-1
222. Yu Y., Yang T., Ma P., et al. (2025). Determining the status of tertiary lymphoid structures in invasive pulmonary adenocarcinoma based on chest CT radiomic features. *Insights Imaging* **16**:28. DOI:10.1186/s13244-025-01906-w
223. Wu J., Zuo Z., Na L., et al. (2025). Machine learning-driven prediction of intratumoral tertiary lymphoid structures in hepatocellular carcinoma using contrast-enhanced CT imaging and integrated clinical data. *Front. Oncol.* **15**:1652509. DOI:10.3389/fonc.2025.1652509
224. Silva S.B., Wanderley C.W.S., Gomes Marin J.F., et al. (2022). Tumor glycolytic profiling through 18F-FDG PET/CT predicts immune checkpoint inhibitor efficacy in advanced NSCLC. Ther. *Adv. Med. Oncol.* **14:**17588359221138386. DOI:10.1177/17588359221138386.
225. Siska P.J., Singer K., Evert K., et al. (2020). The immunological warburg effect: Can a metabolic-tumor-stroma score (MeTS) guide cancer immunotherapy. *Immunol. Rev.* **295**:187–202. DOI:10.1111/imr.12846
226. Yan Y., Zou X., Lin X., et al. (2025). Assessment of tertiary lymphoid structures via 18F-FDG PET/CT scan in patients with pancreatic adenocarcinoma. *Cancer Immunol. Immunother.* **74**:345. DOI:10.1007/s00262-025-04205-x
227. Long S., Li M., Chen J., et al. (2025). Transfer learning radiomic model predicts intratumoral tertiary lymphoid structures in hepatocellular carcinoma: A multicenter study. *J. Immunother. Cancer* **13**:e011126. DOI:10.1136/jitc-2024-011126
228. Wang T., Wang L., Zhong H., et al. (2025). MRI-derived radiomics model for predicting intratumoral tertiary lymphoid structures in soft tissue sarcoma. *Insights Imaging* **16**:201. DOI:10.1186/s13244-025-02086-3
229. Li K., Ji J., Li S., et al. (2024). Analysis of the correlation and prognostic significance of tertiary lymphoid structures in breast cancer: A radiomics-clinical integration approach. *J. Magn. Reson. Imaging* **59**:1206–1217. DOI:10.1002/jmri.28900
230. Lin Y., Yu Y., Wang Q., et al. (2025). Machine learning model for predicting tertiary lymphoid structures and treatment response in triple-negative breast cancer. *Npj Precis. Oncol.* **9**:216. DOI:10.1038/s41698-025-01012-6
231. Xu Y., Li Z., Zhi W., et al. (2025). An MRI-based model for preoperative prediction of tertiary lymphoid structures in patients with gallbladder cancer. *Insights Imaging* **16**:189. DOI:10.1186/s13244-025-02007-4
232. Liu L., Gao F., Li Y., et al. (2025). An interpretable radiomics-based model using susceptibility-weighted imaging for non-invasive prediction of tertiary lymphoid structures in hepatocellular carcinoma. *J. Hepatocell. Carcinoma* **12**:2197–2211. DOI:10.2147/JHC.S551462
233. Ma L., Liao S., Zhang X., et al. (2025). Application of intravoxel incoherent motion in the prediction of intra-tumoral tertiary lymphoid structures in hepatocellular carcinoma. *J. Hepatocell. Carcinoma* **12**:383–398. DOI:10.2147/JHC.S508357
234. Li Y., Li X., Xiao X., et al. (2025). A novel hybrid model for predicting tertiary lymphoid structures and targeted immunotherapy outcomes in hepatocellular carcinoma: A multicenter retrospective study. *Eur. Radiol.* **35**:3206–3222. DOI:10.1007/s00330-024-11255-9
235. Xu Y., Li Z., Yang Y., et al. (2024). Association between MRI radiomics and intratumoral tertiary lymphoid structures in intrahepatic cholangiocarcinoma and its prognostic significance. *J. Magn. Reson. Imaging* **60**:715–728. DOI:10.1002/jmri.29128
236. Meyer M., Ronald J., Vernuccio F., et al. (2019). Reproducibility of CT radiomic features within the same patient: Influence of radiation dose and CT reconstruction settings. *Radiology* **293**:583–591. DOI:10.1148/radiol.2019190928
237. Midya A., Chakraborty J., Gönen M., et al. (2018). Influence of CT acquisition and reconstruction parameters on radiomic feature reproducibility. *J. Med. Imaging* **5**:011020. DOI:10.1117/1.JMI.5.1.011020
238. Stamoulou E., Spanakis C., Manikis G.C., et al. (2022). Harmonization strategies in multicenter MRI-based radiomics. *J. Imaging* **8**:303. DOI:10.3390/jimaging8110303
239. Crombé A., Kind M., Fadli D., et al. (2020). Intensity harmonization techniques influence radiomics features and radiomics-based predictions in sarcoma patients. *Sci. Rep.* **10**:15496. DOI:10.1038/s41598-020-72535-0
240. Tan C., Huang J., Gao N., et al. (2025). Dynamic remodeling of tertiary lymphoid structures in response to cancer therapy: A recent review. *Cancer Immunol. Immunother. CII* **74**:313. DOI:10.1007/s00262-025-04183-0

FUNDING AND ACKNOWLEDGMENTS

This work was supported by grants from the National Natural Science Foundation of China (Grant No. 82273083), the National Natural Science Foundation of China (Grant No. 82272733), the National Key Laboratory of Druggability Evaluation and Systematic Translational Medicine (Grant No. QZ23-9), and the Tianjin Key Medical Discipline Construction Project (Grant No. TJYXZDXK-3-004B). The funders had no role in study design, data collection and analysis, decision to publish, or preparation of the manuscript.

AUTHOR CONTRIBUTIONS

All authors contributed to the manuscript and approved the final version.

DECLARATION OF INTERESTS

The authors declare no competing interests.

DATA AND CODE AVAILABILITY

No new data were created or analyzed in this study.